Relativistic LCAO with Minimax Principle and New Balanced Basis Sets

Inaugural-Dissertation
zur Erlangung des
akademischen Grades eines
Doktors der Naturwissenschaften
(Dr. rer. nat.)

vorgelegt beim Fachbereich
Naturwissenschaften, Universität Kassel

von
Hui Zhang
aus Emei, China

1. Gutachter: Prof. Dr. D. Kolb
2. Gutachter: Prof. Dr. M. Lein

Tag der mündlichen Prüfung: 25. November 2008

2

Ich widme diese Arbeit allen meinen Lehrern
von der Vorschule ab bis heute

Contents

List of Tables

List of Figures

Chapter 1

Introduction

In the investigation of systems containing heavy elements (in atoms, molecules, solids), it is important to take relativistic effects into consideration [1, 2]. Therefore an increasing number of relativistic calculations have been made in the last two decades [1, 2]. For this purpose, it is crucial to have efficient schemes for obtaining energy optimized approximate solutions to the one particle Dirac equations and further to relativistic many particle problems. But one encounters great difficulties by variational methods when solving the Dirac equation for molecules with sufficiently high accuracy, if one constructs a relativistic procedure analogous to the non-relativistic case.

Different from the non-relativistic Schrödinger operator, the Dirac Hamiltonian is unbound from below, i.e., the expectation value of the Dirac Hamiltonian with a trial function is not bounded from below by the exact ground state of the system, which causes the so called "variational collapse". In order to avoid this difficulty, it is essential to project against negative continuum (positronic) contributions for positive energy (electronic) states. There are several options for projection: via boundary conditions, with balanced bases, new functionals (e.g. minimax energy functional), etc. A projection via bound states asymptotic behaviors is practical for atomic, but not for molecular calculations.

It is already known that one needs to establish certain relations between the large and small components bases for projection purposes. One important approximation of such treatments is the well known kinetic balance method, which has a correct non-relativistic limit and has been widely applied with different basis sets (even-tempered, contracted, restricted or unrestricted, etc.). However it is not perfectly safe [3, 4] and does not ensure variational upper bounds, especially for systems containing heavy elements. In order to completely get rid of spurious states and contaminated states caused by "variational collapse", we looked for better approaches beyond kinetic balance (KB).

Visscher et al. introduced an "atomic balance" technique [5, 6], where the large and small

components of atomic solutions are used as balanced basis pairs. Atomic balanced basis sets are preferred for inner shell molecular orbitals, additional unrestricted KB basis for the valence region. As both kinds of balanced basis sets for molecular valence orbitals are applied together, this leads to an enlarged small component basis set which might be quite linear dependent and its size has to be reduced to some extent in practical calculations. Systematically constructed balanced basis sets were not available.

The minimax idea originates from Talman [7], and the variational upper bound for the ground-state electron solution was proven by Dolbeault et al. [8, 9, 10] mathematically, even for a more general class of potentials including the strong Coulomb potential. The principle is equivalent to a constraint minimization of the expectation value of the Dirac Hamiltonian. Thus, one can get the positive energy spectrum of the Dirac equation only, without spurious states and spurious positronic admixture, by minimizing a two-component minimax functional. In practical calculations [11], LaJohn and Talman did much to improve the calculations with the minimax principle [7], the ground state energy still happens to be lower than the exact value in one case and a spurious state below the ground state occurred in two cases. So in present research the safety of the minimax principle from Dolbeault et al. [8] will be investigated on one-electron systems with the linear combination of atomic orbitals (LCAO) method, in short, minimax LCAO. The numerical atomic relativistic orbitals (AOs) [12] are used in our calculations, instead of Slater Type Orbitals (STOs) or Gaussian Type Orbitals (GTOs).

Although the minimax LCAO shows the variational safety in our investigated systems, a disadvantage is the non-linear energy dependence of the minimax energy functional. Thus, one consumes a lot of time on matrix element calculations and diagonalizations, as one has to iterate the eigenenergy in the denominator of the kinetic energy term. Furthermore one eigenvalue after the other has to converged starting from the lowest in order not to miss a nearby eigenvalue. Since standard eigenvalues are provided by the minimax LCAO, it helps us to develop possible kinetic energy functionals which are not dependent on the eigenvalue. In present work, several energy functionals with different constructions of the small component bases are investigated and compared to the minimax LCAO, using the same large component basis set, by which the main incompleteness error is given (obtained from a comparison to the more accurate finite element method (FEM) results). We find that the projection error against negative continuum contributions varies sensitively with different constructions of the small spinor components. During the investigation of methods, the benchmark values for one-electron systems are provided by Kullie et al. with the two-component FEM minimax method [13, 14, 15] and from his previous four-component FEM calculations [16, 17].

The further important research is the application of the linear methods on multi-electron systems, both in chemistry simulations and ion-atom scattering physics. Since Rosén and Ellis [12] developed a relativistic LCAO code for general molecular systems, the accuracy

was increased and density functional theory (DFT) included [18, 19, 20, 21] over the years. Although Sepp and Fricke [22] considered the error of this method small given the requirements at that time, we wanted to improve it with a more rigorous principle and remove spurious states, which influence the calculational stability and even worse are an obstacle to dynamic relativistic formulations.

First, in multi-electron chemistry, the benchmarks of Wang [23] and Kullie [24] provide a standard of spectroscopic constants for the systems Ag_2, Au_2, Rg_2, and encourage research in our scheme to construct large relativistic basis sets for high accuracy. The investigation of Wang [23] on the basis convergence also helps to scrutinize the contribution of every basis function. With the large basis set in heavy and super-heavy systems we will investigate and compare the traditional four-spinor method and the new linear balance methods.

Second, multi-electron correlation diagram calculations [25, 26, 27, 28, 29] were applied for the ion-atom scattering dynamic research. Short internuclear distance situations form highly relativistic super-heavy quasi-molecules. It is interesting, for example, at short internuclear distances to look at the phenomena of variational problems, and test the variational safety and projection power of the different methods.

Chapter 2

Relativistic Model

2.1 One electron Dirac equation

When molecules involve small atoms, the Schrödinger equation is a good approximation. But if heavy and super-heavy atoms are contained in molecular systems, the Dirac equation is necessary to describe the properties of the systems, namely, the relativistic effects. Before getting into many-electron systems, the one electron Hamiltonian with its solutions and properties will be shown here.

The one electron Dirac Hamiltonian is written as following,

$$\hat{H} = c\,\hat{\boldsymbol{\alpha}} \cdot \hat{\mathbf{p}} + mc^2\hat{\beta} + \hat{V} \tag{2.1}$$

where $\hat{\boldsymbol{\alpha}}$ and $\hat{\beta}$ are Dirac Matrices:

$$\hat{\boldsymbol{\alpha}} = \begin{pmatrix} 0 & \hat{\boldsymbol{\sigma}} \\ \hat{\boldsymbol{\sigma}} & 0 \end{pmatrix}, \quad \hat{\beta} = \begin{pmatrix} I & 0 \\ 0 & -I \end{pmatrix} \tag{2.2}$$

and the Pauli matrices are:

$$\hat{\boldsymbol{\sigma}} = \begin{pmatrix} 0 & 1 \\ 1 & 0 \end{pmatrix} \cdot \mathbf{e_1} + \begin{pmatrix} 0 & -i \\ i & 0 \end{pmatrix} \cdot \mathbf{e_2} + \begin{pmatrix} 1 & 0 \\ 0 & -1 \end{pmatrix} \cdot \mathbf{e_3} \tag{2.3}$$

$\mathbf{e_i}$, $i = 1, 2, 3$ are the three unit vectors. And $\hat{\mathbf{p}}$ is the momentum operator, c the speed of light. Atomic units are used throughout, $\hbar = m = e = 1$ with $c = 137.0359895$. The Dirac equation is therefore a four by four matrix equation or a group of four coupled differential equations. And the solutions are four-component spinors. The one-electron Dirac equation then is:

$$H \begin{pmatrix} \psi_1 \\ \psi_2 \\ \psi_3 \\ \psi_4 \end{pmatrix} = \lambda \begin{pmatrix} \psi_1 \\ \psi_2 \\ \psi_3 \\ \psi_4 \end{pmatrix} \tag{2.4}$$

The solution of the Dirac equation for one electron consists of the positive and negative continuum spectrum and bound states. In order to understand why all electrons do not fall down from positive states into the negative continuum, all negative states are assumed to be filled and this is taken as the vacuum. When an electron jumps to a positive state from the negative continuum with an additional energy, a positive energy electron and a hole in the vacuum are found. This hole is a positron.

Except for quite simple potentials, no exact analytic solution is available, one needs numerical methods, like finite difference or finite basis methods. Within a finite basis set the Ritz variational principle is used to construct the electron spectrum. The variational functional is

$$I = \langle \psi \mid c\,\hat{\boldsymbol{\alpha}} \cdot \hat{\mathbf{p}} + mc^2 \hat{\beta} + \hat{V} - (E + mc^2) \mid \psi \rangle \tag{2.5}$$

where by an energy shift $\lambda = E + mc^2$, E corresponds to nonrelativistic energy in the non-relativistic limit $c \to \infty$.

Searching for the lowest positive state energy with a finite basis, the Ritz method leads to a solution mixed with negative states, unless the projection against the negative continuum is made. Without projection the searched energy is unbounded from below. One might chose a suitable basis set or find some constraints, or even transform Dirac Hamiltonian into another Hamiltonian in order to avoid this problem.

2.2   Solution for one electron Atom

In a spherical (central) potential the one-electron solutions can be written as

$$\phi_{n\kappa\mu} = \begin{pmatrix} \frac{P_{n\kappa}(r)}{r} \chi_{\kappa\mu}(\theta, \phi) \\ i \frac{Q_{n\kappa}(r)}{r} \chi_{-\kappa\mu}(\theta, \phi) \end{pmatrix} \tag{2.6}$$

where $\chi_{\kappa\mu}(\theta, \phi)$ is a vector coupled function of a spherical harmonic $Y_{l\mu-\sigma}(\theta, \phi)$ and a spin function φ_σ

$$\chi_{\kappa\mu}(\theta, \phi) = \sum_{\sigma=-\frac{1}{2}}^{\frac{1}{2}} C(l, \frac{1}{2}, j, \mu - \sigma, \sigma) Y_{l,\mu-\sigma}(\theta, \phi) \varphi_\sigma \tag{2.7}$$

$C(l, \frac{1}{2}, j, \mu - \sigma, \sigma)$ are the Clebsch-Gordon coefficients and the spin functions are

$$\varphi_{\frac{1}{2}} = \begin{pmatrix} 1 \\ 0 \end{pmatrix}, \varphi_{-\frac{1}{2}} = \begin{pmatrix} 0 \\ 1 \end{pmatrix} \tag{2.8}$$

The Dirac quantum number κ is given by

$$\kappa = \begin{cases} -(j + \frac{1}{2}) = -(l+1) & for \quad j = l + \frac{1}{2} \\ (j + \frac{1}{2}) = l & for \quad j = l - \frac{1}{2} \end{cases} \tag{2.9}$$

where j is the total angular momentum quantum number, μ is the projection of j. And for hydrogen-like atoms, the radial wave function is of the form

$$r^{\gamma-1} e^{-\lambda r} P(r) \tag{2.10}$$

where $P(r)$ is polynomial of r, and γ and λ are, respectively,

$$\gamma = (\kappa^2 - (\alpha Z)^2)^{1/2} \tag{2.11}$$

and

$$\lambda = c^{-1}[-E(-E + 2mc^2)]^{1/2} \tag{2.12}$$

and the energy is

$$E = mc^2(1 + \frac{(\alpha Z)^2}{(\sqrt{\kappa^2 - (\alpha Z)^2} + n')^2})^{-1/2} \tag{2.13}$$

with $\alpha = 1/c$, $n' = 0, 1, 2, ...$

2.3 Multi-electron relativistic method

In a system with N nuclei and K electrons, the Hamiltonian includes the kinetic energy operators of the nuclei and electrons, and the Coulomb interactions between electrons and nuclei, electrons and electrons, nuclei and nuclei. With the coordinates R_k of nuclei and r_i of electrons, it is expressed as following,

$$\hat{\boldsymbol{H}}_{\boldsymbol{D}} = \sum_{k=1}^{K} T_k + \sum_{i=1}^{N} \left(c\,\hat{\boldsymbol{\alpha}} \cdot \hat{\boldsymbol{p}}_i + m_e c^2 \hat{\beta} \right) - \sum_{i=1}^{N} \sum_{k=1}^{K} \frac{Z_k}{|\mathbf{r_i} - \mathbf{R_k}|} + \sum_{i<j}^{N} \frac{1}{|\mathbf{r_i} - \mathbf{r_j}|} + \sum_{k<l}^{K} \frac{Z_k Z_l}{|\mathbf{R_k} - \mathbf{R_l}|} \tag{2.14}$$

The Breit interaction, which describe the electromagnetic interaction between two moving electrons, is neglected, for we mainly focus on the variational method and its problems.

The corresponding quantum equation is

$$H\Psi = E\Psi \tag{2.15}$$

where Ψ is the eigen function of all electron and nuclear coordinates, E is the total energy of the system. In order to simplify the problem, approximations are made.

2.4   The Born-Oppenheimer approximation

As the nuclei move much slower than electrons, the kinetic energy of them could be omitted. Thus the left Hamiltonian H_{el} has only the kinetic and potential energy of electrons. The repulsion between nuclei is now fixed and is included in the total energy of the systems after solving the electron equation. And the wavefunction of the total system could be taken as a product of wavefunctions of the electrons and nuclei,

$$\Psi = \psi_{el}(\mathbf{r}, \mathbf{R})\psi_{nuc}(\mathbf{R}) \tag{2.16}$$

where in $\psi_{el}(\mathbf{r}, \mathbf{R})$ $\mathbf{R}$ (position of nuclei) are parameters, not coordinates like in $\psi_{nuc}(\mathbf{R})$. The quantum equation,

$$H_{el}\psi_{el}(\mathbf{r}, \mathbf{R}) = E_{el}\psi_{el}(\mathbf{r}, \mathbf{R}) \tag{2.17}$$

is solved with the normalization constraint,

$$\langle \psi_{el}(\mathbf{r}, \mathbf{R}) \mid \psi_{el}(\mathbf{r}, \mathbf{R}) \rangle = 1 \tag{2.18}$$

2.5   Dirac-Fock method

The multi-electron wavefunction is approximated by a Slater determinant of a set of ortho-normalized single electron spin wavefunctions

$$\mathbf{\Psi}(\mathbf{r}_1, \mathbf{r}_2, \cdots) = \frac{1}{\sqrt{N!}} \begin{vmatrix} \boldsymbol{\psi}_1(\mathbf{r}_1) & \boldsymbol{\psi}_1(\mathbf{r}_2) & \cdots & \boldsymbol{\psi}_1(\mathbf{r}_N) \\ \boldsymbol{\psi}_2(\mathbf{r}_1) & \boldsymbol{\psi}_2(\mathbf{r}_2) & \cdots & \boldsymbol{\psi}_2(\mathbf{r}_N) \\ \cdots & \cdots & \cdots & \cdots \\ \boldsymbol{\psi}_N(\mathbf{r}_1) & \boldsymbol{\psi}_N(\mathbf{r}_2) & \cdots & \boldsymbol{\psi}_N(\mathbf{r}_N) \end{vmatrix} \tag{2.19}$$

Then the expecting value of the Hamiltonian is

$$
\begin{aligned}
E_{tot} &= \langle \boldsymbol{\Psi} \mid \hat{\boldsymbol{H}} \mid \boldsymbol{\Psi} \rangle \\
&= E_{nuc} + \sum_{i=1}^{N} \int \boldsymbol{\psi}_i^{\dagger}(\mathbf{r}_i)\hat{h}(\mathbf{r}_i)\boldsymbol{\psi}_i(\mathbf{r}_i)d^3\mathbf{r}_i \\
&\quad + \frac{1}{2}\sum_{i,j=1}^{N} \int\int \boldsymbol{\psi}_i^{\dagger}(\mathbf{r}_i)\boldsymbol{\psi}_j^{\dagger}(\mathbf{r}_j)\frac{1}{r_{ij}}\boldsymbol{\psi}_i(\mathbf{r}_i)\boldsymbol{\psi}_j(\mathbf{r}_j)d^3\mathbf{r}_i d^3\mathbf{r}_j \\
&\quad - \frac{1}{2}\sum_{i,j=1}^{N} \int\int \boldsymbol{\psi}_i^{\dagger}(\mathbf{r}_i)\boldsymbol{\psi}_j^{\dagger}(\mathbf{r}_j)\frac{1}{r_{ij}}\boldsymbol{\psi}_i(\mathbf{r}_j)\boldsymbol{\psi}_j(\mathbf{r}_i)d^3\mathbf{r}_i d^3\mathbf{r}_j \quad (2.20)
\end{aligned}
$$

With the variational method and the orthogonal constraint

$$
\int \boldsymbol{\psi}_i^{\dagger}(\mathbf{r})\boldsymbol{\psi}_j(\mathbf{r})d^3\mathbf{r} = \delta_{ij}
$$

one can get a set of coupled integro-differential equations

$$
(\hat{\boldsymbol{h}}_{\boldsymbol{i}} + V^H + V^X + V_{nuc})\boldsymbol{\psi}_i(\mathbf{r}_i) = \varepsilon_i \boldsymbol{\psi}_i(\mathbf{r}_i) \quad (2.21)
$$

where V^X is defined as the exchange potential by

$$
V^X(\mathbf{r}_i)\boldsymbol{\psi}_i(\mathbf{r}_i) = -\sum_{j=1}^{N}\int \boldsymbol{\psi}_j^{\dagger}(\mathbf{r}_j)\frac{1}{r_{ij}}\boldsymbol{\psi}_i(\mathbf{r}_j)\boldsymbol{\psi}_j(\mathbf{r}_i)d^3\mathbf{r}_j \quad (2.22)
$$

The Dirac-Fock method is the base of other methods to describe correlations of electrons, such as the multi-configuration method (MC) , the configuration interaction method (CI), etc. And the Kohn-Sham equation in density functional theory is also derived with a single determinant of a non-interacting multi-electron system.

Chapter 3

Minimax Principle and LCAO

3.1   Talman's work

Talman [7] introduced a minimax principle as following to avoid the negative continuum problem in a variational method

$$\lambda = \inf_{\psi_+} \; \sup_{\psi_-} \frac{\langle \psi \mid \hat{H} \mid \psi \rangle}{\langle \psi \mid \psi \rangle} \tag{3.1}$$

the ψ_+ and ψ_- are the two large and small components of the four-component spinor ψ (in short, four-spinor) respectively. One may obtain the ground state by minimization over ψ_+ and maximization over ψ_- .

3.2   Dolbeault's work

Dolbeault et al [9, 10] proposed another minimax principle

$$\lambda_k = \inf_{\substack{dimG=k \\ G \text{ subspace of } F_+}} \; \sup_{\substack{\psi \neq 0 \\ \psi \in (G \oplus F_-)}} \frac{\langle \psi \mid \hat{H} \mid \psi \rangle}{\langle \psi \mid \psi \rangle} \tag{3.2}$$

where $F_+ \oplus F_-$ is an orthogonal decomposition of a well chosen space of square integrable functions.
And they also proposed an energy functional [8, 36] with the constraint minimization (definition of the functional I is the left side of the following equation)

$$\int \frac{|\hat{L}\psi_+|^2}{E + 2mc^2 - V} d^3\mathbf{r} + (V - E)\,|\psi_+|^2 d^3\mathbf{r} = 0 \tag{3.3}$$

where $L = c\,\hat{\sigma} \cdot \hat{\mathbf{p}}$ and σ_k, $(k = 1, 2, 3)$ are the Pauli matrices. This principle has been proven by Dolbeault et al. [10] to be mathematically equivalent to the minimax principle and has the same positive spectrum as the four-spinor Hamiltonian in a Coulomb potential, even though in equation (3.3) only a variation of the two large components ψ_+ is necessary. In the following, we sketch how to arrive at equation (3.3).

The first step is to eliminate the two small components ψ_- from the Dirac equations, which are four coupled first order differential equations,

$$\hat{L}\psi_+ = (E + 2mc^2 - V)\psi_- \tag{3.4}$$

$$\hat{L}^\dagger\psi_- = (E - V)\psi_+ \tag{3.5}$$

One resolves equation (3.4) for ψ_- and inserts into equation (3.5) leaving a relation for two large components ψ_+ alone. Then multiply by $\psi_+^\dagger$ from the left and integrate. The step of eliminating the two small components is known, but it is usually followed by an expansion with respect to a certain small number, for instance, $1/c$. The non-linear functional was not derived before and investigated for its properties. There exits a unique E satisfying equation (3.3) for a given admissible ψ_+ (for which the integral in the equation is well defined), taking it as $E[\psi_+]$. Minimization over ψ_+ will determine the ground state, (in short, two-spinor for the large two-components spinor ψ_+)

$$E_1 = \min_{\psi_+} E[\psi_+] \tag{3.6}$$

3.3   LCAO method

Solving the molecular problem, expansions in discrete basis sets with various sorts of functions are used, as well as numerical grid point methods: Gaussian Type Orbitals (GTO) [30], Slater Type Orbitals (STO) [7, 31, 11], numerical atomic orbitals (AOs) [12, 18, 19, 20, 21], Finite Element Method (FEM) [32, 33, 34, 35, 16, 17, 13] , B-spline[36].

3.3.1   Four-spinor LCAO

In the linear combination of atomic orbitals (LCAO) method, the molecular functions are expanded as a sum of four-component spinors:

$$\psi_i^{MO} = \sum_j c_{ij}\, \chi_j^{AO} \tag{3.7}$$

This turns the energy functional I in equation 2.5 into a function of the c_{ij}. Minimization with respect to c_{ij} gives a matrix equation

$$H\,X \;=\; \epsilon\,S\,X \tag{3.8}$$

H and S are the Hamiltonian and the overlap matrix, respectively. As all four components are applied, we call it traditional four-component spinor LCAO (in short, (traditional) four-spinor LCAO) to distinguish it from minimax two-component spinor LCAO and four-component spinor LCAO with balanced bases.

3.3.2   Two-spinor minimax LCAO

With the minimax energy functional 3.3, the linear combination of the large two-component spinors, only,

$$\psi_{i+}^{MO} = \sum_j c_{ij}\,\chi_{j+}^{AO} \tag{3.9}$$

leads to a similar matrix equation. This method will be called minimax two-component spinor LCAO (in short, minimax two-spinor LCAO).

3.3.3   Difference of the small component in LCAO

Both the two-spinor LCAO and the traditional four-spinor LCAO [12] schemes use the same large components χ_{j+}^{AO} of the AO basis, the small components however are different: in the two-spinor LCAO approach it will always follow (although it will not appear in the functional, it is needed in wavefunction and density calculations)

$$\psi_{i-}^{MO} := \sum_j c_{ij} \cdot \frac{\hat{L}\chi_{j+}^{AO}}{(E_i^{MO} + 2mc^2 - V^{MO})} \tag{3.10}$$

while in the traditional four-spinor LCAO approach one keeps the atomic small components, i.e.

$$\psi_{i-}^{MO} := \sum_j c_{ij} \cdot \frac{\hat{L}\chi_{j+}^{AO}}{(E_j^{AO} + 2mc^2 - V_j^{AO})} \tag{3.11}$$

3.3.4   Property

The advantage of the numerical atomic orbital basis is that atomic orbitals are good approximations for inner (core) molecular orbitals (MOs), and have the correct behavior close to the nuclei. AOs also approximate well high lying MOs where the potentials of the different atomic sites are mainly seen through their monopole contribution with respect

to the total charge center (in quasi-molecular calculations, see the basis construction in Chapter 3.5).

But in chemistry calculations for bond properties the basis sets of valence atomic orbitals may be small, and more basis sets (ionized atoms of the same or different elements) are required to achieve chemistry accuracy (see the basis construction in Chapter 5). Worth to mention that different type basis sets (for the molecular valence orbitals) could be utilized in combination with numerical AOs, for example, with FEM basis [34], or STO basis [37, 23]

3.4   Minimax FEM approach

An important application of the minimax principle is with the finite element method (FEM) [13], which offers very accurate values for relativistic theoretical studies. Four-spinor FEM of Yang's work [38, 32] as benchmark was cited by many authors [39]. In order to avoid problems of four-spinor FEM (one sees in Düsterhöft's research [40] (for multi-electron system with heavy element calculation could be very hard to converge within four-spinor FEM scheme), Kullie made two-spinor minimax FEM and achieved success with high accuracy and better convergence behavior. For more details be referred to [16, 17, 13, 41, 24]

3.5   Results of two-spinor minimax LCAO

3.5.1   Basis construction with parameter

Before showing the results, a basis construction method is introduced here. To construct an AO basis, which is particularly suited for the quasi-molecular case, the atomic potential for a given center i includes the monopole contributions from all other atoms' potentials: if r_i is the electron distance to center i, R_{ij} the distance from nuclear center i to j, then the AO basis potential is chosen

$$V_i^{AO} = -\frac{Z_i}{r_i} + V^{mon} \tag{3.12}$$

$$V_{r_i \leq R_{ij}}^{mon} = \sum_{j \neq i} -\frac{Z_j}{R_{ij}}, \quad r_i \leq R_{ij}\,; \qquad V_{r_i > R_{ij}}^{mon} = \sum_{j \neq i} -\frac{Z_j}{r_i}, \quad r_i > R_{ij} \tag{3.13}$$

In addition, the basis sets centered at the nuclei are complemented by a molecular monopole potential with respect to the common charge center, because this is good for all the orbitals where $R_{ij} \ll r_e$, the radius of the electronic orbitals, especially for high

angular momentum states, which in addition are always quite non-relativistic. For these states one thus obtains, as expected, almost the same good convergence behavior in the traditional four-spinor scheme as in the two-spinor minimax formulation.

The draw-back of the monopole potential construction of equation(3.13) is that it is not differentiable in contrast to the real potentials which worsens the numerics and the negative continuum contributions. In order to improve the basis further a nonlinear parameter β is introduced for the construction of the potential,

$$V_{new}^{mon}(r_i) = \sum_{j \neq i} -\frac{Z_j}{R_{ij}} e^{-(\beta r_i)^2} + \sum_{j \neq i} -\frac{Z_j}{r_i}(1 - e^{-(\beta r_i)^2}) \tag{3.14}$$

This is different from the idea of LaJohn [11], who used a nonlinear parameter α in the form $e^{-\alpha r}$ for the decay tail of wavefunctions. Varying the new parameter β, one can strongly affect the influence of the negative continuum and obtain better results with smaller bases. Although the idea is simple and one could introduce other parameters and shapes of basis sets, we wanted to improve the basis in a simple and transparent way. The atomic orbitals are calculated by solving the atomic Dirac equation numerically with proper boundary conditions. The electronic AOs are thus accurately projected with respect to the AO negative continuum at their center i. As the molecular negative continuum differs from a superposition of the AO continua, one faces a breakdown of the AO pre-projection. It is obvious that any means that bring the MO and AO (negative) continuum contributions closer to each other will improve the accuracy and diminish the influence of the MO negative continuum onto the LCAO electronic states.

Table 3.1: The ground state energy relative error of H$_2^+$ with different β, Δ_4 error 4-spinor, Δ_2 error 2-spinor scheme, basis 3d3d3d. The 'true [16]' value is **1.1026415810336** a.u.

β	Δ_4	Δ_2
0.1	1.38629×10^{-3}	1.38587×10^{-3}
0.2	3.2883×10^{-4}	3.2896×10^{-4}
0.3	4.9208×10^{-4}	4.9163×10^{-4}
0.4	7.6324×10^{-4}	7.6283×10^{-4}
0.5	5.9184×10^{-4}	5.9218×10^{-4}
0.6	1.9007×10^{-4}	1.8994×10^{-4}
0.7	3.5150×10^{-4}	3.5108×10^{-4}
0.8	1.47063×10^{-3}	1.47031×10^{-3}
0.9	2.74394×10^{-3}	2.74361×10^{-3}

Table 3.2: The ground state energy relative error of Th_2^{179+} with different β, Δ_4 error 4-spinor, Δ_2 error 2-spinor scheme, basis 3d3d3d. The 'true [13]' value is **-9504.7567469**6 a.u.

β	Δ_4	Δ_2
10	1.920×10^{-3}	1.875×10^{-3}
20	2.4×10^{-4}	6.6×10^{-4}
30	1.8×10^{-4}	6.8×10^{-4}
40	1.3×10^{-3}	8.9×10^{-4}
50	-8.8×10^{-4}	4.9×10^{-4}
60	-1.8×10^{-3}	3.6×10^{-4}
70	-5.27×10^{-3}	5.79×10^{-4}
80	5.1×10^{-3}	1.2×10^{-3}
90	1.27×10^{-3}	1.83×10^{-3}

3.5.2   Discussion of Minimax LCAO Result

All calculations on Th_2^{179+} were done at a scaled H_2^+ distance $R = 2/90$ a.u. (for H_2^+, $R = 2$ a.u.), thus the non-relativistic energies of Th_2^{179+} would just be the one for H_2^+ multiplied by Z^2 ($Z = 90$). With comparison of two systems Th_2^{179+} and H_2^+, one could both achieve relativistic effect, and investigate the phenomena between light and heavy quasi-molecules. Varying the basis parameter β, where the basis includes $1s$ up to $3d$ at all centers (two centers at nuclei, one at common charge center), in Tables 3.1 and 3.2 comparisons are made between the two-spinor minimax and the traditional four-spinor variational scheme for H_2^+ and Th_2^{179+}, respectively. Boldface digits in energy values of both captions are the high accurate values from finite element method (FEM) calculation [16].

We see in Table 3.1 that for light system like H_2^+, where relativistic effects are small, the ground state in a four-spinor scheme is contaminated rather little, the results of the two-spinor minimax and traditional four-spinor schemes are nearly the same. And there are no spurious states.

In Table 3.2, spurious states appear in the four-spinor LCAO calculation, but there are no spurious states in the two-spinor minimax scheme. As expected, Table 3.2 shows that the traditional four-spinor LCAO approach gives solutions which are contaminated by negative continuum contributions, while the two-spinor minimax results never fall below the true value and are generally the closest to it.

A best choice of the parameter β becomes less crucial in the two-spinor minimax scheme the bigger the AO basis; we take $\beta = 60$ for all basis sets. Another good reason to make this parameter choice is the lowest state energy of the atomic orbitals. For $\beta = 60$, this

atomic energy is close to the lowest molecular energy, whereas for other values of β and for the case without β (normal monopole potentials) this is not so. That means, this basis has a correct decay tail $e^{-\alpha r}$, where $\alpha \approx 154$, which was also used in LaJohn's work [11], for the correct decay behavior of the molecular orbital when r is large,

$$\alpha = c^{-1}[-E(-E + 2mc^2)]^{1/2} \tag{3.15}$$

But note from equation (3.14) that our parameter β serves the more general purpose in also significantly affecting the basis behavior around the other center.

Table 3.3 gives the convergence of the ground- and first-excited state, comparing the potential equation (3.14) and the normal monopole potential equation (3.12). The values are in accord with the results of FEM, GTO, STO and B-Spline calculations.

Table 3.3: 2-spinor ground and first excited state energies with the β dependent multi-centered AO basis potentials for $\beta = 60$ and the normal monopole ones for varying basis sizes (two and three centers).

basis	**E (a.u.) with 2 type of potentials** with $\beta = 60$		normal monopole	
	$\epsilon_{1s_{1/2g}}$	$\epsilon_{1s_{1/2u}}$	$\epsilon_{1s_{1/2g}}$	$\epsilon_{1s_{1/2u}}$
3d3d	-9449.51	-6802.59	-9419.84	-6796.94
3d3d3d	-9501.37	-6813.53	-9457.40	-6804.01
3d4f3d	-9501.83	-6813.99	-9472.65	-6805.49
3d5g3d	-9501.95	-6814.08	-9479.32	-6806.57
3d6h3d	-9502.02	-6814.11	-9482.42	-6807.06
4f4f4f	-9502.63	-6814.19	-9488.20	-6808.76
4f6h4f	-9502.86	-6814.27	-9494.11	-6810.22
5g5g5g	-9503.18	-6814.50	-9496.14	-6811.32
5g6h5g	-9503.25	-6814.55	-9497.35	-6812.57
6h6h6h	-9503.55	-6814.64	-9498.27	-6813.48
FEM	**-9504.756746923** [16]	**-6815.5132**180 [17]		
STO [11]	-9504.7497 †			
STO [31]	-9476.7	-6773.4		
GTO [30]	-9504.756696 ‡			
B-Spline [36]	-9497.51			

† in that paper, they have for $n_{max} = 4$ and $l_{max} = 3$ the contaminated energy -9504.9805 and for $n_{max} = 5$ one spurious state.
‡ 60s/50p/40d/30f/20g/10h/2i basis set with R = 2/90 bohr.

The two-spinor minimax LCAO's results are worse than FEM, since FEM could use a

big number of elements and points, appropriate coordinate transformations for partial regularization of the nuclear singularity, and vary all components of the spinor (two components in minimax two-spinor FEM, four components in four-spinor FEM, respectively) freely, while in our LCAO case we have only one coefficient. However, without special coordinate transformations as FEM, LCAO has no particular difficulty with multi-centered calculations.

The result in Ref. [11] is also better than our LCAO. In our calculation, different basis states have different decay tails (for example, the $1s$ atomic orbital decay tail is close to that of the molecular ground state, only), because atomic orbitals contain all kinds of states, high lying and low lying. While in the calculation [11] with STO basis sets, all basis states have the same α, say 154, best suited for the ground state. For other molecular states α should change. In this sense, they use a much bigger basis than we do and they have to search for each excited state with a different α. This way one might easily miss almost degenerate energy states. We will discuss below our LCAO approach which guarantees to obtain the complete spectrum up to a certain excitation energy. We will also show that with the nonlinear two-spinor functional equation (3.3) no spurious nor contaminated states occur in contrast to the work of LaJohn et al. [11].

In Tables 3.4, 3.5, 3.6 we give a more complete comparison for the computed spectrum of Th_2^{179+} for two-spinor minimax LCAO and traditional four-spinor LCAO as well as two-spinor minimax FEM and four-spinor FEM.

In the two-spinor minimax approach one has the basic problem that one may miss an energy level since a non-linear iteration over the eigenvalue is needed in order to solve equation (3.3). In the present two-spinor minimax LCAO approach this could only be solved by successive construction in the following way: first the ground-state energy is converged where a direct solver (Householder diagonalization) diagonalizes eq. (3.3) for a fixed value of E in the kinetic term on the left side since in this case equation (3.3) defines a linear homogeneous eigenvalue problem. E is then iteratively updated by the diagonalized energy value $E_1^{(n)}$, (n = iteration count) which is always closer to the true energy than $E_1^{(n-1)}$. After E_1 converged, one looks for the next higher energy $E_2^{(0)}$, keeping E_1 in the denominator of the kinetic term in equation (3.3). $E_2^{(0)}$ is only a first guess for E_2, but it is assured that there is no other eigenvalue between them (even after convergence of $E_2^{(n)}$ by successive update for E in the kinetic term of equation (3.3)). This holds because our LCAO basis set provides a rather uniformly good approximation to all sufficiently low lying molecular states. A direct diagonalization generates the whole spectrum for the given basis and thus assures that no energy level is missing, which might happen with iterative solvers if there are almost energeticly degenerate levels of the same symmetry. In fact in the FEM calculations which have to use iterative solvers it was only possible to find the complete spectrum after rather accurate LCAO values were available. In a four-spinor approach which defines a linear eigenvalue problem one may easily guarantee

finding all eigenvalues by counting the diagonal elements in a Cholesky decomposition of the shifted matrix in an inverse vector iteration scheme [42].

Of course, having to construct, in the two-spinor minimax LCAO, the complete set of molecular (or quasi-molecular) eigenvalues and wavefunctions, both the complete diagonalization (rather than iterative solver) for each orbital and the nonlinear iteration steps for a given orbital makes the calculation orders of magnitude more expensive than the traditional four-spinor LCAO scheme. Because the traditional four-spinor LCAO needs only one diagonalization for the entire spectrum, with the same matrix sizes as in two-spinor minimax LCAO, making it a lot less time-consuming. This rather unsatisfactory situation of the two-spinor minimax LCAO is at present unavoidable, if one wants to be sure to solve the relativistic problem free of spurious and free of contaminated states without missing a level.

There are opposing trends in LCAO and FEM accuracies as seen quite clearly in Tables 3.4, 3.5, 3.6 and this may be understood: the higher the excitation energy the better the AO basis generally becomes, because the MOs approach the center of charge monopole AOs. On the other hand in the two center FEM numerical scheme one starts loosing, because the higher the excitation energy the fewer points are available per local wavelength of the orbitals which become more and more oscillatory both in radial and angular direction.

In contrast to two coefficients for each spinor component in two-spinor minimax FEM, the two-spinor minimax LCAO has only one coefficient. This difference does not affect the behavior of projection against the negative continuum: similar as two-spinor minimax FEM, the two-spinor minimax LCAO results convergence from above and do not show spurious nor contaminated states. Thus there obviously is no need for independent variation of the two large components to avoid contamination. This may be understood from the minimax principle equation (3.2) where one projects onto positive energy states irrespective how good the approximating space G is chosen. However for further improved accuracy of two-spinor LCAO energies, especially for the low lying levels, it might be necessary to vary both large components independently.

There is a striking difference to FEM of the behavior of four-spinor LCAO, which exhibits many spurious states in the low lying spectrum and a few for higher excitation energies, in addition to many contaminated ones. In four-spinor FEM where all 4-spinor components vary freely, there are no spurious nor significantly contaminated states in the low lying spectrum, but one already knows that spurious states may show up in the higher lying excitation spectrum where these spurious states only slowly move up out of the interesting spectrum with increased numbers of points (improved accuracy) [34, 40].

Tables 3.4, 3.5, 3.6 show in comparison of LCAO and FEM values that for certain high lying states LCAO is very accurate whenever, for small j_z, 2- and 4-spinor LCAO energies agree nicely, indicating that the AO basis is rather complete for these states. For higher j_z where only higher angular momentum AOs can contribute, the orbitals become more

non-relativistic and thus 2- and 4- spinor values automatically agree closer. In this case the agreement of 2- and 4- spinor energies is not a good indicator for completeness of the AO basis any more. Spurious states do not necessarily give deeper contaminated energies for nearby levels, but could also lead to less bound values. A detailed analysis of the AO contributions in the molecular orbitals exhibits the expected property that the LCAO values are the more accurate the less low angular momentum two center AOs contribute to the MO. These localized AOs can not be constructed sufficiently well by simple monopole type atomic potentials; the influence of higher AO multi-polarities is needed but then one loses the simple factorization properties into radial and angular parts of the AOs. Though perhaps advantageous the construction of such AO bases would be considerably more complicated and is out of the scope of our presently available relativistic AO code ("multipole" AOs).

Table 3.4: Spectrum of $J_z = 1/2$ states Th$_2^{179+}$ up to $n = 6$. s marks spurious; d, dd, h, hh contaminated states (d: deeper, dd: much deeper than 'true (FEM)' energies; h: higher, hh: much higher than 2-spinor LCAO).

		E (a.u.)			
		LCAO(6h6h6h)		FEM	
No.	J_z	2-spinor	4-spinor	2-spinor	4-spinor
	1/2		-53160.1 s		
	1/2		-46810.2 s		
	1/2		-45252.2 s		
	1/2		-44278.9 s		
	1/2		-39893.3 s		
	1/2		-38287.2 s		
	1/2		-36175.6 s		
	1/2		-32671.0 s		
	1/2		-31245.5 s		
	1/2		-24182.2 s		
	1/2		-19086.3 s		
	1/2		-12353.7 s		
	1/2		-10777.4 s		
1	1/2	-9503.55	-9510.50 dd	**-9504.75674696** [13]	**-9504.756746923** [16]
2	1/2	-6814.64	-6813.20 h	-6815.513203 [a]	**-6815.513218**0 [c]
	1/2		-5850.30 s		
3	1/2	-4126.79	-4126.48 h	-4127.890868 [a]	
	1/2		-4028.39 s		
4	1/2	-3373.53	-3374.23	-3374.519985 [a]	**-3374.520003**4 [c]
5	1/2	-2563.80	-2563.11 h	-2564.180730 [a]	**-2564.1807300** [c]
6	1/2	-2455.31	-2457.08 d	-2455.956176 [a]	**-2455.956258**1 [c]
7	1/2	-2010.44	-2010.01 h	-2010.663504 [a]	**-2010.6635076** [c]
8	1/2	-1916.45	-1917.072	-1917.123897 [a]	**-1917.123931**8 [c]
9	1/2	-1652.34	-1655.06 d	-1652.815226 [a]	**-1652.815249**0 [c]
	1/2		-1352.10 s		
10	1/2	-1336.51	-1336.46 h	-1336.674352 [a]	**-1336.6743**699 [c]
11	1/2	-1329.93	-1292.28 hh	-1330.25545 [a]	**-1330.25550**52 [c]
	1/2		-1173.49 s		
12	1/2	-1138.82	-1138.42 h	-1138.97815 [a]	**-1138.9781703** [c]
13	1/2	-1105.034	-1105.162 d	-1105.11161 [a]	
14	1/2	-1083.80	-1084.36 d	-1084.18180 [a]	

– Continued from previous page

| | | E (a.u.) | | | |
| | | LCAO(6h6h6h) | | FEM | |
No.	J_z	2-spinor	4-spinor	2-spinor	4-spinor
15	**1/2**	-1055.782	-1055.780 h	-1055.80218 [a]	
16	**1/2**	-966.380	-965.694 d	-966.60706 [a]	
17	**1/2**	-818.980	-819.154 d	-819.14152 [b]	
18	**1/2**	-815.257	-815.272	-815.33611 [a]	
19	**1/2**	-723.295	-723.502 d	-723.38925 [a]	
20	**1/2**	-706.322	-706.480 d	-706.38210 [b]	
21	**1/2**	-691.818	-693.190 d	-692.03717 [a]	
22	**1/2**	-679.705	-679.913 d	-679.72285 [b]	
23	**1/2**	-675.3442	-675.3447	-675.34591 [b]	
24	**1/2**	-662.76429	-662.76487 d	-662.76469 [b]	
	1/2		-633.577 s		
25	**1/2**	-630.276	-630.196 h	-630.39384 [a]	
26	**1/2**	-551.337	-551.827 d	-551.42844 [b]	
27	**1/2**	-547.374	-547.624 d	-547.41980 [b]	
	1/2		-544.820 s		
28	**1/2**	-497.352	-497.835 d	-497.41005 [b]	
29	**1/2**	-487.753	-487.843 d	-487.79259 [b]	
30	**1/2**	-478.242	-478.127 h	-478.37306 [b]	
31	**1/2**	-471.984	-471.903 h	-471.99673 [b]	
32	**1/2**	-469.4005	-469.40177	-469.40262 [b]	
33	**1/2**	-461.99060	-461.99168 d	-461.99112 [b]	
34	**1/2**	-461.10330	-461.10327 h	-461.10357 [b]	
35	**1/2**	-456.49378	-456.49358 h	-456.49399 [b]	
36	**1/2**	-442.240	-442.284	-442.30431 [b]	

[a] 7th order FEM, grid points $N = 3249$, singular transformation $\nu = 4$;
[b] singular transformation $\nu = 2$ [17];
[c] [13]

Table 3.5: Spectrum of $J_z = 3/2$ states Th_2^{179+} up to $n = 6$. s marks spurious; d, h, hh contaminated states (d: deeper than 'true (FEM)' energies, h: higher, hh: much higher than 2-spinor LCAO).

		E (a.u.)		
		LCAO(6h6h6h)		FEM
No.	J_z	2-spinor	4-spinor	2-spinor [a]
	3/2		-46369.5 s	
	3/2		-38372.4 s	
	3/2		-36205.0 s	
	3/2		-32841.7 s	
	3/2		-10368.5 s	
	3/2		-7045.25 s	
1	3/2	-3652.95	-3647.85 hh	-3653.567953
2	3/2	-2009.36	-2008.42 h	-2009.642338
3	3/2	-1872.55	-1872.70	-1872.872588
4	3/2	-1769.13	-1768.11 h	-1769.552971
5	3/2	-1126.90	-1126.65 h	-1127.062519
6	3/2	-1088.474	-1088.499	-1088.511464
7	3/2	-1070.09	-1070.73 d	-1070.323206
8	3/2	-1048.892	-1048.938 d	-1048.911084
9	3/2	-1022.23	-1022.31	-1022.465956
	3/2		-885.701 s	
	3/2		-809.122 s	
10	3/2	-714.623	-714.148 h	-714.707575
11	3/2	-696.409	-696.405 h	-696.439812
12	3/2	-685.950	-685.857 h	-686.084597
13	3/2	-675.805	-675.786 h	-675.821905
14	3/2	-673.9003	-673.8971 h	-673.901848
15	3/2	-661.91081	-661.91095	-661.911188
16	3/2	-660.564	-660.133 h	-660.701865
	3/2		-543.357 s	
17	3/2	-491.605	-491.518 h	-491.651778
18	3/2	-481.576	-481.5888	-481.597689
19	3/2	-475.221	-475.401 d	-475.299198
20	3/2	-469.612	-469.562 h	-469.624198
21	3/2	-468.5092	-468.51150 d	-468.511090
22	3/2	-461.47196	-461.47229	-461.472453
23	3/2	-460.84660	-460.84661	-460.846838
24	3/2	-460.306	-460.281 h	-460.388737
25	3/2	-456.32182	-456.32168 h	-456.321993

[a] 7th order FEM, grid points $N = 3249$, singular transformation $\nu = 2$

Table 3.6: Spectrum of $J_z = 5/2$ to $11/2$ states Th_2^{179+} up to $n = 6$. s marks spurious; d, h contaminated states (d: deeper than 'true (FEM)' energies, h: higher than 2-spinor LCAO).

		E (a.u.)		
		LCAO(6h6h6h)		FEM
No.	J_z	2-spinor	4-spinor	2-spinor [a]
	5/2		-30364.6 s	
1	**5/2**	-1791.37	-1791.681 d	-1791.620132
	5/2		-1607.90 s	
	5/2		-1439.59 s	
2	**5/2**	-1063.76	-1063.77	-1063.874773
3	**5/2**	-1036.811	-1036.810 h	-1036.832410
4	**5/2**	-1033.88	-1033.967	-1034.069035
5	**5/2**	-682.691	-682.703	-682.788469
6	**5/2**	-671.0885	-671.0885	-671.090002
7	**5/2**	-669.118	-669.123	-669.138191
8	**5/2**	-667.087	-667.274 d	-667.206186
9	**5/2**	-660.25059	-660.25091	-660.251093
10	**5/2**	-473.347	-473.363	-473.410158
11	**5/2**	-466.7891	-466.790546	-466.790640
12	**5/2**	-465.593	-465.6154 d	-465.607097
13	**5/2**	-464.248	-464.477 d	-464.324749
14	**5/2**	-460.46626	-460.466959 d	-460.466869
15	**5/2**	-460.33531	-460.33525	-460.335492
16	**5/2**	-455.98083	-455.98077 h	-455.980973
1	**7/2**	-1023.077	-1023.079	-1023.147301
2	**7/2**	-666.967	-666.968	-667.008251
3	**7/2**	-661.688	-661.692	-661.752026
4	**7/2**	-657.8757	-657.8761	-657.881967
5	**7/2**	-464.233	-464.234	-464.315746
6	**7/2**	-461.186	-461.190	-461.224915
7	**7/2**	-459.57312	-459.57307 h	-459.573255
8	**7/2**	-459.024	-459.025	-459.038686
9	**7/2**	-455.476988	-455.476916 h	-455.477083
1	**9/2**	-654.951	-654.951	-654.982302
2	**9/2**	-458.5541	-458.5540 h	-458.564319
3	**9/2**	-457.231	-457.231	-457.300956
4	**9/2**	-454.8189	-454.8189	-454.823106
1	**11/2**	-454.0165	-454.0164 h	-454.026322

[a] 7th order FEM, grid points $N = 3249$, singular transformation $\nu = 2$ [17]

Chapter 4

Balance Method

The minimax energy functional equation (3.3) was proven to have the same positive energy spectrum $E + mc^2$ as the Dirac Hamiltonian [8], but the eigenvalues in the denominator are not known in advance. If one wants to avoid having to iterate them, one has to either make an approximation of the Hamiltonian or project differently from equation (3.3) against the negative continuum, e.g. project via orthogonality to a properly discretized negative continuum. Such a discretization may be obtained by a specially constructed small component basis and introducing additional expansion coefficient for the small components of the four-spinor. This is not a minimax method, but a four-spinor scheme with coefficients c_{ij} and d_{ij} for the large and small component basis, respectively. We discuss several possibilities.

4.1   Kinetic Balance (KB)

First we simplify the denominator (equation 3.10) such that only the $2mc^2$ is left, which one readily notices to be the well known Kinetic Balance (KB). The expansions for the large and small components are

$$\psi_{i+}^{MO} \;=\; \sum_j c_{ij}\, \chi_{j+}^{AO}, \tag{4.1}$$

$$\psi_{i-}^{MO} \;=\; \sum_j d_{ij}\, \frac{\hat{L}\chi_{j+}^{AO}}{2mc^2}. \tag{4.2}$$

Inserting them into the Dirac energy functional equation (2.5), one gets an eigenvalue equation in doubled space

$$H^d\, X^d \;=\; E\, S^d\, X^d. \tag{4.3}$$

In Kinetic Balance formulation there is no energy and potential dependence in the denominator, so one can easily apply it in general molecular calculations, however, at the expense of rather poor accuracy as we will show the following results.

4.2   Molecular Balance (TVB)

In order to go beyond that, a natural extension is using the molecular potential in the denominator, which in particular has all the molecular potential V^{MO} singularities in every small component basis

$$\psi_{i-}^{MO} = \sum_j d_{ij} \frac{\hat{L}\chi_{j+}^{AO}}{(E_0 + 2mc^2 - V^{MO})}.$$ (4.4)

The E_0 in equation(4.4) is a constant. Instead of E_0 one may use E_j^{AO}, the atomic eigenvalues, which are good for the core and semi-core states, and for excited high lying molecular states (if we construct the atomic potentials by including monopole contributions from all other centers and additionally use the basis set of the eigenstates with the molecular monopole potential with respect to the center of charge). The results show that the molecular eigenvalues are quite insensitive to the choice of E_0. Using the full molecular potential for the construction of the small component basis set it may be called Molecular Balance or Kinetic and Potential Balance (TVB).

4.3   Defect Balance (TVDB)

Inspecting the derivation of the minimax functional equation(3.3) one notices that two of the four Dirac equations are resolved exactly. If we iteratively resolve these two Dirac equations up to terms quadratic in $1/(E_0 + 2mc^2 - V^{MO})$, we get a new basis set, which may be called Kinetic and Potential Defect Balance (TVDB)

$$\psi_{i-}^{MO} = \sum_j c_{ij} \frac{\hat{L}\chi_{j+}}{E_0 + 2mc^2 - V^{MO}} + \sum_j d_{ij} \frac{\hat{L}\chi_{j+}}{(E_0 + 2mc^2 - V^{MO})^2}.$$ (4.5)

One can see that the first term would be identical to traditional four-spinor LCAO if one replaced V^{MO} by V_j^{AO} and E_0 by E_j^{AO}. The remainder in equation(4.5) is of third order in $1/(E_0 + 2mc^2 - V^{MO})$, while the error of TVB is of second order in it. Although in TVB there are already no spurious states, the defect basis set improves the accuracy further.
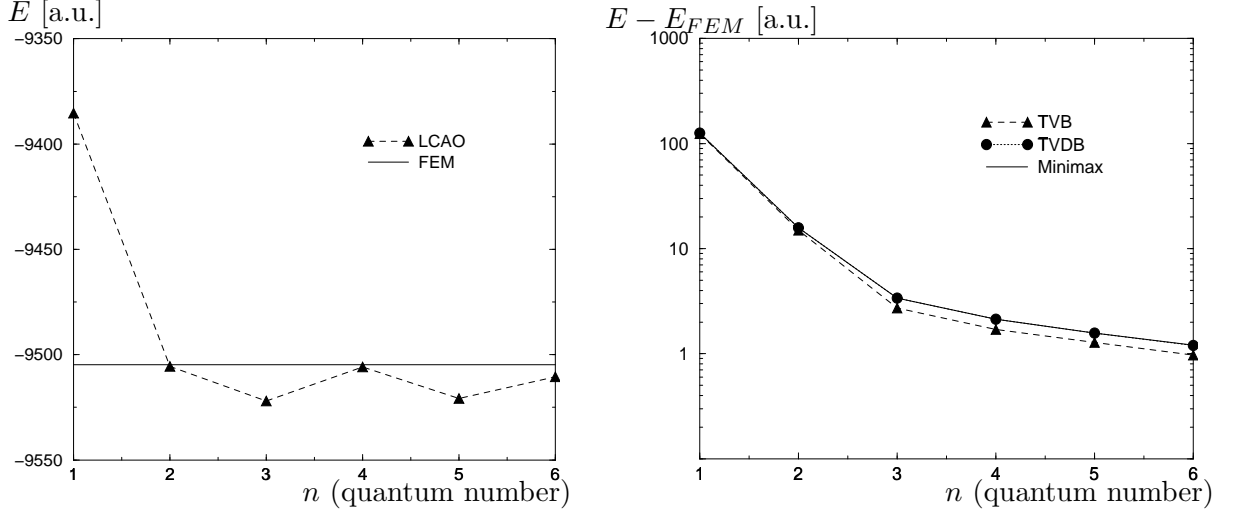
Figure 4.1: Th_2^{179+} $1s_{1/2}\sigma_g$ energy, convergence behavior of various methods. All states n_1l_1, n_2l_2, n_3l_3 where the n_i run up to a given n and $l_i = 0$ up to $n_i - 1$ form the 3 center basis (with modified atomic potential $\beta = 60$ [14]), $E_0 = -4000$ for TVB and TVDB (Left: LCAO); (Right: TVB, TVDB and Minimax.)

4.4 Discussion of Approximation Method

We calculate the highly relativistic quasi-molecular one electron system Th_2^{179+} with KB, TVB, and TVDB methods and compare them with four-spinor LCAO, and two-spinor Minimax LCAO results. The AOs are constructed from atomic potentials which include modified monopole potential contributions from the other center(s) with $\beta = 60$ [14]. Figure 4.1 is a comparison of the ground state energy with increasing basis size n_1l_1, n_2l_2, n_3l_3 (3 center basis). n_i denote the principal quantum numbers which run up to n, where $n = 1$ to 6. All states up to a given n with angular momenta $l_i = 0$ to $n_i - 1$ form the 3 center basis. The left part shows the traditional four-spinor LCAO results. The straight line in the middle is the FEM value -9504.757 for comparison. The right part shows the TV Balance, TV Defect Balance and Minimax LCAO energy differences to the highly accurate FEM result and their convergence behavior. Note the different scales to show the behavior more clearly. We see that the error of LCAO is much bigger than of TVB and TVDB and it does not converge, because of the weaker projection properties. The results of TVB, TVDB and Minimax LCAO converge monotonically to the FEM value, and TV and TV Defect Balance are lower than Minimax LCAO, within drawing accuracy TVDB and Minimax LCAO are indistinguishable. Being deeper and thus closer to the true value does not mean they are better than Minimax LCAO, for we know that Balance projection is worse. TVB and TVDB converge to the Minimax LCAO values, the difference between them becomes smaller with basis size increase, mainly following a power law $n^{-1.5}$, n being the maximal principal quantum number. This is not to be

Table 4.1: Spectrum of $J_z = 1/2$ energies in a.u. Th_2^{179+} ($R = 2/90$ a.u.) for 3-centered AO basis set $n = 3$ (see fig. 1 and text, atomic potentials with modified monopole contributions from other centers [14]). s marks spurious. $E_0 = -4000$ a.u.

No.	4-SP LCAO	KIN-B	T-V-B	T-V-D-B	MINIMAX	FEM [14]
	-22144 s	-13257 s				
		-11910 s				
1	-9522	-8902	-9502.03	-9501.3736	-9501.3702	-9504.757
		-8348 s				
2	-6815.1	-7382	-6813.68	-6813.5240	-6813.5238	-6815.513
		-4541 s				
3	-4123.6	-3995	-4121.44332	-4121.4432495	-4121.4432495	-4127.891
4	-3402	-3219	-3369.7294	-3369.7277640	-3369.7277639	-3374.520
	-3042 s					
5	-2564.7	-2380	-2562.640	-2562.632276	-2562.632273	-2564.181
6	-2477	-2334	-2446.961	-2446.952315	-2446.952310	-2455.956
	-2217 s					
7	-1997.0	-1996.9	-2005.9662	-2005.9650440	-2005.9650433	-2010.664
8	-1914.6	-1878	-1911.382	-1911.372274	-1911.372260	-1917.124
9	-1650.15	-1618	-1650.458	-1650.449831	-1650.449822	-1652.815

confused with the convergence behavior in fig. 4.1, which addresses the approximation error as a function of n.

To show the phenomena in detail we give four tables with different basis sizes comparing several linear approximations to Minimax LCAO and the results of traditional four-spinor LCAO, Minimax LCAO and FEM. In the last Chapter 3.5 we focused on showing the success of two-spinor Minimax LCAO. Here our main purpose is by a detailed comparison to investigate the behavior of the new linear methods. The rather large number of digits given in the tables are meant to exhibit the difference of the various approaches within the same numerics. The integration accuracy is such that the largest errors on norms are 10^{-8}, but often the errors stay below 10^{-9}. The relative accuracies of the energy values for the given basis sets are of similar order except for spurious and low accuracy states where the errors may be orders of magnitude bigger. In these states integration errors are obviously strongly enhanced.

We find that KB has spurious states not only below the ground state but also in the spectrum. For the bases ($n = 4$ and $n = 5$) it is difficult in KB to decide which states are spurious and which not (x marks in the table). Occurrence of the spurious states indicates an insufficient projection ability against negative continuum contributions in this highly

Table 4.2: Spectrum of $J_z = 1/2$ energies in a.u. Th_2^{179+} ($R = 2/90$ a.u.) for 3-centered AO basis set $n = 4$ (see fig. 1 and text, atomic potentials with modified monopole contributions from other centers [14]). s marks spurious. x means: it can not be decided that this energy is spurious or not, which makes the level assignment only tentative. $E_0 = -4000$ a.u.

No.	4-SP LCAO	KIN-B	T-V-B	T-V-D-B	MINIMAX	FEM [14]
	-25624 s	-14187 s				
	-25563 s	-12027 s				
1	-9505.8	-9382 x	-9503.06	-9502.632	-9502.6293	-9504.757
2	-6819.5	-7131 x	-6814.27	-6814.18987	-6814.18974	-6815.513
	-5167 s	-5727 x				
3	-4130.0	-4042	-4124.94545	-4124.9454024	-4124.9454024	-4127.891
		-3453 s				
4	-3376.8	-3218	-3372.4089	-3372.4077166	-3372.4077165	-3374.520
5	-2562.8	-2391	-2563.0357	-2563.031269	-2563.031267	-2564.181
6	-2465	-2376	-2454.6440	-2454.638815	-2454.638813	-2455.956
7	-2012.5	-1997	-2009.7020	-2009.7008474	-2009.7008467	-2010.664
8	-1917.8	-1891	-1914.9396	-1914.932827	-1914.932817	-1917.124
9	-1653.7	-1628	-1651.8514	-1651.845769	-1651.845762	-1652.815
10	-1339.8	-1311	-1335.9597	-1335.953872	-1335.953865	-1336.674
11	-1336.7	-1296	-1329.693	-1329.685476	-1329.685467	-1330.255
12	-1173	-1131.4	-1138.3659	-1138.364079	-1138.364076	-1138.978
13	-1105.5	-1103.5	-1104.6254	-1104.624850	-1104.624849	-1105.112
14	-1087.6	-1074	-1083.043	-1083.036800	-1083.036780	-1084.182
	-1084 s					
15	-1055.70	-1055.66	-1055.67602	-1055.6760082	-1055.6760081	-1055.802
16	-965.9	-959.3	-966.0699	-966.065786	-966.065777	-966.6071

relativistic situation within our AO basis. Only when Z/c goes to zero the projection will become perfect. This has been found in our tests for the light system H_2^+, where no spurious states occur with KB. Another point is that KB results are more accurate for high-lying than low-lying states, partly because the high-lying states are less relativistic and thus one has a good projection possibility, and partly because the high-lying kinetic balanced AOs have little strength in the core region where the potential varies strongly. The fluctuations in energies with basis size are unsystematic and unpredictable. It was already mentioned in [6] that calculations with relativistically contracted large components basis sets supplemented by kinetically balanced small components may diverge for the ground state. The missing potential dependence of the small component basis in KB

may be simulated to some extend by superposition of a larger basis. This might explain the fair success in [6] where the small components of atomic solutions for the inner shell orbitals are combined with KB for the other orbitals.

The traditional four-spinor LCAO results on average are much better than KB (even though more spurious states appear and intrude into the spectrum), because the four-spinor AOs are on average the better physical basis. The traditional four-spinor LCAO approach is best when the internuclear distance is big because then the AOs do not overlap much and thus the pre-projection of the AOs is quite well preserved in LCAO. And when used with a minimal basis set, which however does not give good accuracy, the pre-projection also does not deteriorate much, the artifacts remain small, in particular no spurious states occur.

TV Balance results are much better than traditional four-spinor LCAO. Compared to KB, the accuracy is better because of the improved construction of the small component basis at the atomic centers. And compared to traditional four-spinor LCAO one has the additional freedom of doubled coefficients. This improves the projection property, as the negative continuum is discretized naturally with the help of the balanced basis.

TV Balance is quite close to Minimax LCAO results, which is the proper standard for the chosen AO large component basis, instead of comparing to the highly accurate FEM values. Because, we should distinguish between the truncation error due to a finite basis size and the projection properties against the negative continuum by various kinds of balanced constructions of the small component basis with the same large component basis choice. These projection properties one infers from a comparison to Minimax LCAO results which are perfectly projected against the negative continuum.

The sensitivity of TVB on the energy E_0 is weak, one may replace it by E_j^{AO}, the atomic energies, and obtain results of similar quality, at least in our basis set. It will be of great practical importance to explore the sensitivity to the molecular potential in the denominator by replacing the full molecular potential by a number of systematic approximations to it. This seems promising as one may interpret certain results in the literature [43] in this direction.

The TV Defect Balance approach gets us another 2 to 3 digits closer to the Minimax LCAO results, depending on the level, but quite independent of the basis size. This improvement factor between TVB and TVDB generally reflects the same power law convergence of both TVB and TVDB to the minimax values, stated already above. TVB and especially TVDB is a big success over KB and a very promising method with practically almost the same computational effort as the other balance methods, because the relativistic AOs necessitate anyway in numerical integration for the matrix elements. For other type large component basis sets it might be advantages to re-fit the small component basis space in terms of a similar class of functions as used for the large components and then the effort will be enhanced. The defect part of the small component basis in particular allows

both to discretize the negative continuum for projection and exhaust the large component approximation power of the atomic basis: among the linear approximations to Minimax LCAO here TVDB is the best. But one may argue that the projection error, which is orders of magnitude smaller than the truncation error, indicates that the projection quality is overdone and could be considerably worsened, even for such a super-heavy system like Th_2^{179+}. This offers the possibility to save computational effort (by a smaller number of d_{ij} till the projection error increases to the order of the approximation error). It will be of great practical importance to see how far one can thus push the effort towards that of four-spinor LCAO, which is minimal in a given relativistic AO basis size.

Table 4.3: Spectrum of $J_z = 1/2$ energies in a.u. Th_2^{179+} ($R = 2/90$ a.u.) for 3-centered AO basis set $n = 5$ (see fig. 1 and text, atomic potentials with modified monopole contributions from other centers [14]). s marks spurious. x means: it can not be decided that this energy is spurious or not, which makes the level assignment only tentative. $E_0 = -4000$ a.u.

No.	4-SP LCAO	KIN-B	T-V-B	T-V-D-B	MINIMAX	FEM [14]
	-20155 s	-14089 s				
	-12536 s	-11712 s				
	-12055 s					
1	-9521	-10741 x	-9503.48	-9503.1836	-9503.18198	-9504.757
	-7481 s	-7673 x				
2	-6813.95	-7580 x	-6814.536	-6814.50083	-6814.50076	-6815.513
	-5461 s	-5988 x				
3	-4130.0	-4040	-4126.282956	-4126.2829158	-4126.2829158	-4127.891
	-3666 s					
4	-3379.4	-3294	-3373.1335	-3373.1327366	-3373.1327365	-3374.520
	-2960 s					
5	-2566.3	-2536	-2563.5342	-2563.532099	-2563.532098	-2564.181
6	-2433	-2384	-2455.1141	-2455.109315	-2455.109313	-2455.956
7	-2008.3	-1999	-2010.1863	-2010.1853385	-2010.1853379	-2010.664
8	-1921.0	-1891	-1916.1552	-1916.150317	-1916.150310	-1917.124
9	-1652.58	-1637	-1652.0900	-1652.086366	-1652.086362	-1652.815
	-1432 s					
10	-1326.5	-1328.8	-1336.3751	-1336.372346	-1336.372342	-1336.674
11	-1322.6	-1298	-1329.8603	-1329.853008	-1329.852999	-1330.255
12	-1137.85	-1132.5	-1138.6573	-1138.655940	-1138.655939	-1138.978
13	-1104.72	-1103.8	-1104.8762	-1104.8757458	-1104.8757448	-1105.112
14	-1086.9	-1074.5	-1083.6367	-1083.632415	-1083.632404	-1084.182
	-1065 s					
15	-1055.52	-1055.742	-1055.75025	-1055.7502454	-1055.7502454	-1055.802
16	-966.65	-961.1	-966.2305	-966.227919	-966.227914	-966.6071
17	-818.23	-812.2	-818.9475	-818.942024	-818.942016	-819.1415

Table 4.4: Spectrum of $J_z = 1/2$ energies in a.u. Th_2^{179+} ($R = 2/90$ a.u.) for 3-centered AO basis set $n = 6$ (see fig. 1 and text, atomic potentials with modified monopole contributions from other centers $\beta = 60[14]$). s marks spurious. $E_0 = -4000$ a.u.

No.	4-SP LCAO	KIN-B	T-V-B	T-V-D-B	MINIMAX	FEM [14]
	-36176 s					
	-32671 s					
	-31246 s					
	-24182 s					
	-19086 s					
	-12354 s	-15447 s				
	-10777 s	-13673 s				
1	-9510.50	-8940	-9503.79	-9503.5550	-9503.5538	-9504.757
		-8306 s				
2	-6813.20	-6625	-6814.669	-6814.643698	-6814.643653	-6815.513
	-5850 s					
3	-4126.48	-4032	-4126.787789	-4126.7877545	-4126.7877544	-4127.891
	-4028 s					
4	-3374.23	-3326	-3373.5264	-3373.5258181	-3373.5258177	-3374.520
5	-2563.11	-2706	-2563.8015	-2563.8000129	-2563.8000122	-2564.181
6	-2457.08	-2547	-2455.313	-2455.309632	-2455.309631	-2455.956
		-2033 s				
7	-2010.01	-2004	-2010.4425	-2010.4417540	-2010.4417536	-2010.664
8	-1917.072	-1892	-1916.4569	-1916.452865	-1916.452860	-1917.124
9	-1655.06	-1640	-1652.3456	-1652.342807	-1652.342803	-1652.815
	-1352 s					
10	-1336.46	-1331	-1336.5135	-1336.511389	-1336.511386	-1336.674
11	-1292.28	-1283	-1329.9359	-1329.930772	-1329.930766	-1330.255
	-1173 s					
12	-1138.42	-1135	-1138.8245	-1138.823465	-1138.823463	-1138.978
13	-1105.162	-1104.1	-1105.03453	-1105.034188	-1105.034187	-1105.112
14	-1084.36	-1075	-1083.8081	-1083.804519	-1083.804512	-1084.182
15	-1055.780	-1055.776	-1055.781472	-1055.7814692	-1055.7814692	-1055.802
16	-965.69	-962	-966.3824	-966.380320	-966.380316	-966.6071
17	-819.154	-813	-818.9833	-818.979608	-818.979601	-819.1415

Chapter 5

Chemistry

The interesting element with large relativistic effects, for example Element Au (gold), and light and super-heavy elements in the same column will be investigated within the scheme of Kohn-Sham, including local and nonlocal density functionals, in order to find whether both the traditional four-spinor LCAO and TVDB LCAO work well with chemical distance.

5.1   The Hohenberg-Kohn Theorems

The Hohenberg-Kohn [44] Theorem 1:
The total density of a multi-electron system determines its external potential. In the proof of it, it is clear to find that a contradiction will appear if one density of ground state would relate to two different potentials, thus two different Hamiltonian, and thus leading to two different total energies both for the ground state.
One therefore could represent the total energy of the quantum system as a functional of the total density $E^{total}[\rho(\vec{r})]$,

$$E^{total}[\rho(\vec{r})] \quad = \quad F[\rho(\vec{r})] + \int v_{ext}\rho(\vec{r})d^3\vec{r} \tag{5.1}$$

The great advantage of this density functional is that the functional $F[\rho(\vec{r})]$ is universal (v_{ext} is system specific) and could be easily applied to all large or small systems, if only the formulation of the functional is determined. And it is simple with only a three-dimensional variable, in contrast to the wavefunction of a N-particle system.

The Hohenberg-Kohn Theorem 2:
The total density and total energy of the ground state could be achieved by a variation principle. According to the first theorem, any change of the ground state density will

determine a change in potential, thus in Hamiltonian and wavefunction of the system. The change leads to a new expectation value of the total energy, which is larger than the ground state energy. The variation process with respect to the total density obtains both the ground state density and total energy together.

$$\delta E^{total}[\rho(\vec{r})] \ = \ 0 \tag{5.2}$$

This variational principle is subject to the constraint of total particle number.

$$N \ = \ \int \rho(\vec{r}) d^3\vec{r} \tag{5.3}$$

5.2   The Kohn-Sham Equation

within the Hohenberg-Kohn Theorems, the key points of determination of a multi-particle system are searching the exact density of the system and the energy functional of the density, which is system-independent. A very good idea was introduced by Kohn and Sham [45] that a fictitious system could be investigated if only the density is the same as the system under study. A non-interacting multi-particle system (in an external potential) would be a good and simple choice for this purpose, for which a single Slater determinant is exact to describe the ground state of it. And the kinetic energy functional, one of the difficult parts for interacting systems, is exactly known for such a system as follows, (in the non-relativist case for example $\hat{t} = \frac{1}{2m}\nabla^2$),

$$T_s[\rho(\vec{r})] \ = \ \sum_i^N \langle \Psi_i(\vec{r}) \mid \hat{t} \mid \Psi_i(\vec{r}) \rangle \tag{5.4}$$

where s stands for non-interacting system. The density of such a system is simply the sum of the single-particle density of the orbitals

$$\rho(\vec{r}) \ = \ \sum_i^N \mid \Psi_i(\vec{r}) \mid^2 \tag{5.5}$$

and the corresponding energy is given by

$$E_s^{total}[\rho(\vec{r})] \ = \ T_s[\rho(\vec{r})] + \int v_s \rho(\vec{r}) d^3\vec{r} \tag{5.6}$$

comparing to the density functional of the interacting multi-particle system, one could rearrange the formula 5.1 such that the residual kinetic energy, from the non-interacting kinetic energy could be put into a new part of the potential, the non-classic interaction between electrons as well.

$$E[\rho(\vec{r})] = \int v_{ext}(\vec{r})\rho(\vec{r})d^3\vec{r} + T[\rho(\vec{r})] + V_{ee}[\rho(\vec{r})]$$

$$= \int v_{ext}(\vec{r})\rho(\vec{r})d^3\vec{r} + T_s[\rho(\vec{r})] + E_H[\rho(\vec{r})] + (T[\rho(\vec{r})] - T_s[\rho(\vec{r})] + V_{ee}[\rho(\vec{r})] - E_H[\rho(\vec{r})])$$

$$= \int v_{ext}(\vec{r})\rho(\vec{r})d^3\vec{r} + T_s[\rho(\vec{r})] + E_H[\rho(\vec{r})] + E_{xc}[\rho(\vec{r})] \tag{5.7}$$

the classic repulsion between electron interaction $E_H[\rho(\vec{r})]$ and the exchange and correlation functional $E_{xc}[\rho(\vec{r})]$ are the following respectively,

$$E_H[\rho(\vec{r})] = \int\int \frac{\rho(\vec{r})\rho(\vec{r'})}{|\vec{r} - \vec{r'}|}d^3\vec{r}d^3\vec{r'} \tag{5.8}$$

$$E_{xc}[\rho(\vec{r})] = T[\rho(\vec{r})] - T_s[\rho(\vec{r})] + V_{ee}[\rho(\vec{r})] - E_H[\rho(\vec{r})] \tag{5.9}$$

the application of the variation principle will give the variational equation

$$([c\,\hat{\boldsymbol{\alpha}} \cdot \hat{\mathbf{p}} + mc^2\hat{\beta}] + v_{ext}(\vec{r}) + v_H(\vec{r}) + v_{xc}(\vec{r}))\psi_k(\vec{r}) = \epsilon_k\psi_k(\vec{r}) \tag{5.10}$$

And the Hartree potential and exchange correlation potential are correspondingly derived,

$$v_H(\vec{r}) = \int \frac{\rho(\vec{r'})}{|\vec{r} - \vec{r'}|}d^3\vec{r'} \tag{5.11}$$

$$v_{xc}(\vec{r}) = \frac{\delta E_{xc}[\rho(\vec{r})]}{\delta\rho(\vec{r})} \tag{5.12}$$

By this way one recasts the problem of an interacting system into a non-interacting system with an additional potential V_{xc}. The orbital equations of this fictitious system are called Kohn-Sham [45] equation. Solving the Kohn-Sham equation requires, in the same way as Hartree-Fock procedure, a self-consistent process, namely, the density determines the KS potential, thus the Hamiltonian (with the KS potential) determines the ground state wavefunction, leading to a new density, which will give the next potential. The density functional is not dependent on the molecule, thus it is an *ab initio* method in theoretical physics and chemistry. As the exact form is yet unknown, approximations have to be applied.

5.3   Slater approximation

This approximation is based on the Hartree-Fock (or Dirac-Fock) method mentioned in Chapter 2. It is originally from approximating the exchange part of the Dirac-Fock energy and potential in the following way,

$$V_\alpha^X(\vec{r}) = -\frac{3}{2}\alpha(\frac{3}{\pi}\rho(\vec{r}))^{\frac{1}{3}}, \quad \alpha = 0.7 \tag{5.13}$$

As it is locally dependent on density, it could be taken as one local density functional (it is not the so called local density functional (LDA), which is the next one with both the definition of an exchange and correlation functional). Because it is quite simple, one could take it as a good start for research. (no relativistic version is applied)

5.4   Local density functional

The nonrelativistic local density functional (LDA) consists of the (standard) local exchange functional (LDA), which has the same form as the exact exchange of a homogeneous electron gas (HEG), and the correlation functional, named after Vosko-Wilk-Nusair (VWN) [46]. In the case of large relativistic effects, relativistic corrections to the functionals are taken into account in this investigation [47]. It is called relativistic local exchange functional (RLDA).

$$E_{xc}^{RLDA}(\rho(\vec{r})) \;=\; \int d^3\vec{r}[e_x^{HEG}(\rho(\vec{r}))\phi_{x,0}(\beta) + e_c^{VWN}(\rho(\vec{r}))\phi_{c,0}(\beta)] \tag{5.14}$$

where the homogeneous electron gas exchange functional is,

$$e_x^{HEG}(\rho(\vec{r})) \;=\; -\frac{3(3\pi^2)^{1/3}}{4\pi}\rho^{4/3}(\vec{r}) \tag{5.15}$$

and $\phi_{x,0}$, $\phi_{c,0}$ are the relativistic correction factors of exchange and correlation functional respectively.

5.5   The generalized gradient approximation (RGGA)

A current way to improve the simple functional LDA or RLDA is taking the gradient contribution of the gradient of the density, which includes information of the density of points nearby. This represents non-locality of the system. In this investigation, the Becke(B88) [48] functional for exchange and its relativistic extension (RB88) and the

Perdew(P86) [49] functional for the correlation are applied. The parameter sets of the functionals are referred to the paper [56].

$$E_X^{RGGA}(\rho(\vec{r})) \;=\; \int d^3\vec{r}\, e_x^{HEG}(\rho(\vec{r}))[\phi_{x,0}(\beta) + g_x^{GGA}(\rho(\vec{r}),(\nabla\rho(\vec{r}))^2)\phi_{x,2}(\beta)] \quad (5.16)$$

where $g_x^{GGA}(\rho(\vec{r}),(\nabla\rho(\vec{r}))^2)$ is the gradient contribution and $\phi_{x,2}$ its relativistic extension.

5.6 Density approximation and Hartree potential

5.6.1 Density approximation

As an important contribution of the total energy, the Hartree energy and Hartree potential are required to be accurate enough corresponding to the general accuracy. But the direct calculation of them through three-dimensional integration would be very expensive. The following approximated density for the purpose of effort-saving is made by introducing a set of multi-centered multipole functions [50], which simply leads to one-dimensional integrals only of the Hartree potential over atomic orbitals.
The density is expanded by the following way,

$$\tilde{\rho}(\vec{r}) \;=\; \sum_{K=1}^{N_A}\sum_{j=1}^{M_K}\sum_{l=0}^{Lj}\sum_{m=-l}^{l} Q_{Kjlm}F_{Kj}(\xi_K)Y_{lm}(\theta_K,\phi_K) \quad (5.17)$$

where $\vec{r}$ or (r,θ,ϕ) is in the molecular frame, $\vec{\xi}_K$ or (ξ_K,θ_K,ϕ_K) is in the atomic frame with respect to atomic center K. And fitting functions for the radial part of the atomic density functions are $F_K^j(\xi_K) = [P_j^2(\xi_K)+G_j^2(\xi_K)]$, where $P_j(\xi_K)$ and $G_j(\xi_K)$ are the radial function of the large and small components of the jth wavefunction on center K. Y_{lm} are the real spherical harmonics, and Q_{Kjlm} are the expansion coefficients to be determined. One writes the expansion in short,

$$\tilde{\rho}(\vec{r}) \;=\; \sum_{\nu} q_{\nu}\varphi_{\nu}(\vec{r}) \quad (5.18)$$

$$q_{\nu} \;=\; Q_{Kjlm} \quad (5.19)$$

$$\varphi_{\nu}(\vec{r}) \;=\; F_{Kj}(\xi_K)Y_{lm}(\theta_K,\phi_K) \quad (5.20)$$

ν represents any combination of the indices (K,j,l,m).

5.6.2   Potential expression

The definition of the electron-electron repulsion potential is

$$V_H(\vec{r}) = \int \frac{\rho(\vec{r'})}{|\vec{r} - \vec{r'}|} d^3\vec{r'} \tag{5.21}$$

with a coordinate transformation from the molecular frame $\vec{r}$ to an atomic frame $\vec{\xi}_K$, namely $\vec{r} - \vec{r'} = \vec{\xi}_K - \vec{\xi'}_K$, insertion of the density approximation expression leads to an approximation of the Hartree potential,

$$\tilde{V}_H(\vec{r}) = \sum_{K=1}^{N_A} \sum_{j=1}^{M_K} \sum_{l=0}^{Lj} \sum_{m=-l}^{l} Q_{Kjlm} \int \frac{F_{Kj}(\xi'_K) Y_{lm}(\theta'_K, \phi'_K)}{|\vec{\xi}_K - \vec{\xi'}_K|} d^3\vec{\xi'}_K \tag{5.22}$$

then one proceeds with the expansion of $1/|\vec{\xi}_K - \vec{\xi'}_K|$ in terms of Legendre polynomials

$$\frac{1}{|\vec{\xi}_K - \vec{\xi'}_K|} = \sum_{l'=0}^{\infty} G_{l'}(\xi_K, \xi'_K) P_{l'}(\cos\omega_K) \tag{5.23}$$

where

$$G_{l'}(\xi_K, \xi'_K) = \begin{cases} \frac{\xi'^{l'}_K}{\xi^{l'+1}_K}, & \xi_K \geq \xi'_K \\ \frac{\xi^{l'}_K}{\xi'^{(l'+1)}_K}, & \xi_K < \xi'_k \end{cases} \tag{5.24}$$

and ω_K the angle between $\vec{\xi}_K$ and $\vec{\xi'}_K$. One expands further the Legendre polynomials by real spherical harmonics,

$$P_{l'}(\cos\omega_K) = \frac{4\pi}{2l'+1} \sum_{m'=-l'}^{l'} Y_{l'm'}(\theta_K, \phi_K) Y_{l'm'}(\theta'_K, \phi'_K) \tag{5.25}$$

getting an expression of $1/|\vec{\xi}_K - \vec{\xi'}_K|$ with real spherical harmonics (in angular coordinates) only.

$$\frac{1}{|\vec{\xi}_K - \vec{\xi'}_K|} = \sum_{l'=0}^{\infty} \frac{4\pi}{2l'+1} G_{l'}(\xi_K, \xi'_K) \sum_{m'=-l'}^{l'} Y_{l'm'}(\theta_K, \phi_K) Y_{l'm'}(\theta'_K, \phi'_K) \tag{5.26}$$

One integrates over the angular coordinates θ'_K, ϕ'_K and takes into account the orthogonality of the spherical harmonics.

$$\int Y_{lm}(\theta'_K, \phi'_K) Y_{l'm'}(\theta'_K, \phi'_K) d\Omega'_K = \delta_{ll'}\delta_{mm'} \tag{5.27}$$

Then the approximated Hartree potential shows in terms of real spherical harmonics $Y_{lm}(\theta_K, \phi_K)$ reads

$$\tilde{V}_H(\vec{r}) = \sum_{K=1}^{N_A} \sum_{j=1}^{M_K} \sum_{l=0}^{Lj} \sum_{m=-l}^{l} \frac{4\pi}{2l+1} Q_{Kjlm} Y_{lm}(\theta_K, \phi_K) \tag{5.28}$$
$$\times [\frac{1}{\xi_K^{l+1}} \int_0^{\xi_K} \xi_K'^{(l+2)} F_{Kj}(\xi'_K) d\xi'_K + \xi_K^l \int_{\xi_K}^{\infty} \frac{1}{\xi_K'^{(l-1)}} F_{Kj}(\xi'_K) d\xi'_K]$$

again for convenience, one could use a combination of indices (K, j, l, m).

$$\tilde{V}_H(\vec{r}) = \sum_{\nu} q_{\nu} u_{\nu}(\vec{r}) \tag{5.29}$$

$$u_{\nu}(\vec{r}) = \frac{4\pi}{2l+1} Y_l^m(\theta_K, \phi_K)[\frac{1}{\xi_K^{l+1}} \int_0^{\xi_K} \xi_K'^{(l+2)} F_{Kj}(\xi'_K) d\xi'_K + \xi_K^l \int_{\xi_K}^{\infty} \frac{1}{\xi_K'^{(l-1)}} F_{Kj}(\xi'_K) d\xi'_K]$$

5.6.3 Fitting of the molecular density

A least-square-fit to the SCF iterative density is normally a good way to determine the coefficients of the model density expansion. A more appropriate and better fitting method by minimizing the positive-defined Coulomb energy calculated from the difference of the SCF iterative (true) density and approximated (model) density was introduced [19].

$$\int \int \frac{[\rho(\vec{r}) - \tilde{\rho}(\vec{r})][\rho(\vec{r'}) - \tilde{\rho}(\vec{r'})]}{|\vec{r} - \vec{r'}|} d^3\vec{r} d^3\vec{r'} = min \tag{5.30}$$

with the total charge constraint

$$\sum_{\nu} q_{\nu} \int \varphi_{\nu}(\vec{r}) d^3\vec{r} = Q \tag{5.31}$$

The constraint make the coefficients q_ν linearly dependent. One could eliminate the constraint explicitely by expressing one of them (e.g. the last one q_n) in terms of the other $n-1$ coefficients and get linearly independent $n-1$ coefficients and another approximation form.

$$
\begin{aligned}
\tilde{\rho}(\vec{r}) &= \sum_{\nu=1}^{n-1} q_\nu \left(\varphi_\nu(\vec{r}) - \frac{\int \varphi_\nu(\vec{r_1}) d^3 \vec{r_1}}{\int \varphi_n(\vec{r_1}) d^3 \vec{r_1}} \varphi_n(\vec{r}) \right) + \frac{Q}{\int \varphi_n(\vec{r_1}) d^3 \vec{r_1}} \varphi_n(\vec{r}) \\
&= \sum_{\nu=1}^{n-1} q_\nu \varphi'_\nu(\vec{r}) + Q' \varphi_n(\vec{r})
\end{aligned}
\tag{5.32}
$$

$$
\varphi'_\nu(\vec{r}) = \varphi_\nu(\vec{r}) - \frac{\int \varphi_\nu(\vec{r_1}) d^3 \vec{r_1}}{\int \varphi_n(\vec{r_1}) d^3 \vec{r_1}} \varphi_n(\vec{r})
\tag{5.33}
$$

$$
Q' = \frac{Q}{\int \varphi_n(\vec{r_1}) d^3 \vec{r_1}}
\tag{5.34}
$$

Inserting the new expansion form of the approximation density, one has

$$
\int \int \frac{[\rho(\vec{r}) - \sum_{\nu=1}^{n-1} q_\nu \varphi'_\nu(\vec{r}) - Q' \varphi_n(\vec{r})][\rho(\vec{r'}) - \sum_{\nu=1}^{n-1} q_\nu \varphi'_\nu(\vec{r'}) - Q' \varphi_n(\vec{r'})]}{|\vec{r} - \vec{r'}|} d^3\vec{r} d^3\vec{r'} = min
\tag{5.35}
$$

A linear matrix equation will arise by the variation process with respect to the coefficients of the approximation q_ν, $\nu = 1, 2, ..., n-1$

$$
\underline{\underline{A}} \; \underline{x} \; = \; \underline{b}
\tag{5.36}
$$

$$
A_{\mu\nu} = \int \int \frac{\varphi'_\mu(\vec{r}) \varphi'_\nu(\vec{r'})}{|\vec{r} - \vec{r'}|} d^3\vec{r} d^3\vec{r'} = \int \varphi'_\mu(\vec{r}) u'_\nu(\vec{r}) d^3\vec{r}
\tag{5.37}
$$

$$
b_\nu = \int \int \frac{(\rho(\vec{r}) - Q' \varphi_n(\vec{r})) \varphi'_\nu(\vec{r'})}{|\vec{r} - \vec{r'}|} d^3\vec{r} d^3\vec{r'} = \int (\rho(\vec{r}) - Q' \varphi_n(\vec{r})) u'_\nu(\vec{r}) d^3\vec{r}
\tag{5.38}
$$

$$u'_\nu(\vec{r}) \;=\; \int \frac{\varphi'_\nu(\vec{r'})}{|\vec{r}-\vec{r'}|} d^3\vec{r'} \tag{5.39}$$

And solving the linear equation, getting q_ν, $\nu = 1, 2, ..., n-1$, gives the approximate density (equation 5.18) (or equation 5.32) and Hartree potential (equation 5.29) with q_n.

$$q_n \;=\; \frac{Q}{\int \varphi_n(\vec{r_1})d^3\vec{r_1}} - \sum_{\nu=1}^{n-1} q_\nu \frac{\int \varphi_\nu(\vec{r_1})d^3\vec{r_1}}{\int \varphi_n(\vec{r_1})d^3\vec{r_1}} \tag{5.40}$$

5.7 Basis construction

As we try to find the difference of four-spinor LCAO and TVDB LCAO a reasonable and large enough basis set is necessary to apply, with which good results should be reached close to benchmark values, for example, FEM two-spinor minimax results from Kullie [24] and Beijing Density Functional(BDF) results from Wang and Liu [23].

All our basis sets are constructed by numerical atomic calculation, consisting of a minimal basis set and basis functions from ionized atoms [19, 50, 21, 52]. Minimal basis functions are normally all occupied orbitals of the neutral atoms (slightly ionized atoms are used too in researches [19, 52]). For Ag, it is ($1s_{1/2}$ up to $5s_{1/2}$); for Au, ($1s_{1/2}$ to $6s_{1/2}$); for Rg (element 111), ($1s_{1/2}$ to $7s_{1/2}$). Other basis functions unoccupied have different nodes structure and angular momentum to the valence basis functions (last d- and s- basis in minimal basis set). Ionization leads to a deeper eigenvalue, a bigger exponent, and a shorter radius of the principal maximum. The determination of the ionization degree of the atoms is an optimization procedure for the molecular total energy. The procedure is the following,

- Take a fixed (reasonable) internuclear distance, which is close to the equilibrium bond distance, for the optimization procedure. If the reasonable distance is unknown, one could adopt another way [19, 50, 52]: start from calculating an energy curve for the molecule with the minimal basis set, and take the minimum of the curve as the distance for determination of the ionization for the first additional basis function. A new minimum of the new energy curve with increased basis set is applied for the further process. The distance will change always with increasing basis size and the energy curve calculation is time-consuming. Both methods assume that the ionization degree for the additional basis functions is independent of R.

- All the unoccupied atomic basis functions could be added. Take Au as example, $7s$, $8s$, $9s$ as additional s-type basis; $6p$, $7p$, $8p$ as p-type basis; $6d$, $7d$, $8d$ as d-type

basis; $5f$, $6f$, $7f$ as f-type basis; $5g$, $6g$ as g-type basis; $6h$ as h-type basis. A certain ionization degree will be found for each additional basis function.

- take one basis function search the best degree of ionization for the total energy of the molecule.

- fix the degrees of ionization of all last sub-shells, and search the ionization for the next one.

- continue this procedure one sub-shell after another till the total molecular energy will change only a little (about 0.0001 a.u.).

- the sequence of all additional functions might influence the contribution of each function. We suppose the influence is small.

5.8 Results

The research here with chemical systems is a comparison between traditional four-spinor LCAO and TVDB LCAO calculations, which has nearly the same good results as two-spinor minimax LCAO (as we have seen in Chapter 4) even for super-heavy quasi-molecules. The diatomic molecules, Ag_2, Au_2, Rg_2 are selected, as the relativistic effect of the Au atom is large, and in the eka-gold super-heavy element Rg even larger. Ag as a light element, with similar electron structure as Au, is for reference and comparison. They are standard test models in theoretical chemistry for relativistic calculation. Thus reasonable and as large as possible basis sets, for these dimers, will be found and applied for my comparison.

Some previous research should be mentioned here. Hess and Kaldo [53] made a benchmark investigation of relativistic all-electron coupled-cluster (CCSD(T)) calculation on the gold dimer. The relativistic operator is based on the Douglas-Kroll transformation. i-type functions are found to be needed for satisfactory convergence. For better results the basis set superposition error (BSSE) has to be estimated. Correlating the electrons of the semi-core $5p$ (totally 34 correlated electrons including 6s and 5d shells) gives also non-negligible effect. High accuracy, i.e., R_e within 1 pm, D_e better than 0.1 eV (according to the new experimental value of [54], it differs by 0.15 eV), and ω_e within a few wave numbers was reached.

Wang and Liu [23] searched the optimization of basis functions for Cu_2, Ag_2 and Au_2 at the level of four-component relativistic density functional theory (with standard functional, LDA and GGA(B88/P86)). The basis used is numerical atomic orbitals (NAOs) augmented with additional kinetically balanced Slater-type functions (STFs). According to the convergence behavior with increase of the basis set, for example, change by

0.0048 eV in dissociation energy of Au_2 of LDA with adding h-type function, limits were estimated and suggested to be taken as benchmark for calibrating other calculations of at least for the same density functional, for example, change by 0.0048 eV with adding h-type function . In the research, in conclusion, including up to g-type functions in the basis set is sufficient. And the BSSE did not show a big contribution there. Their LDA results (take Au_2 as example) are 3.1 pm shorter in R_e, 0.74 eV larger in D_e, 8.3 wave numbers lager in ω_e, GGA result is 2.8 pm longer in R_e, 0.07 eV larger in D_e, 11.8 wave numbers lager in ω_e, than the experimental value.

Kullie has done a similar investigation [24] for the benchmark values of the dimers of elements in the group 11, including the super-heavy element Rg, with the safe treatment (minimax method) of the relativistic operator. Although the density functional is only local density functional (nonrelativistic LDA (NLDA), relativistic LDA (RLDA) and Slater functional), the minimax FEM are safe from variational collapse and the finite element basis is more systematic and quite large. The results confirm Wang and Liu's [23].

5.8.1 Relativistic effect in Atoms

The molecular property is related to the corresponding atomic structure. To illustrate the electron structure and relativistic effect of atoms, the valence orbitals of Dirac-Fock-Slater atoms are shown in Table 5.1. One sees easily that

- The structures of all three of them would be nearly the same, if the relativistic effect is not taken into account (the nonrelativistic calculation is made by 10^6 times the speed of light).

- The nonrelativistic $ns_{1/2}$ orbital is much shallower (in energy) than two $(n-1)d$ orbitals (n =5,6,7 for Ag,Au,Rg, respectively), thus it will be surely much involved in binding. And the $(n-1)d_{3/2}$, $(n-1)d_{5/2}$ are degenerate.

- Ag atom's relativistic orbitals do not change much with a small relativistic effect.

- Au atom has nearly the same energy of $6s_{1/2}$ and $5d_{5/2}$.

- Rg atom's $7s_{1/2}$ orbital, with a large relativistic effect, is much deeper than $6d_{5/2}$, even the ground state configuration is changed from $[Rn]6d^{10}7s^1$ to $[Rn]6d^97s^2$.

5.8.2 Smoothness of the Basis

Considering the quality of LCAO molecular results, it is essential to use very accurate and thus highly smooth relativistic atomic orbital solutions. This requires at least ≥ 1500

Table 5.1: Relativistic effect of valence orbitals in atomic Dirac-Fock-Slater calculation (energy in eV).

Ag	$5s_{1/2}$	$4d_{5/2}$	$4d_{3/2}$
rel.	-3.948	-6.622	-7.186
nonrel.	-3.542	-7.315	-7.315
Au	$6s_{1/2}$	$5d_{5/2}$	$5d_{3/2}$
rel.	-5.281	-5.701	-7.244
nonrel.	-3.668	-7.467	-7.467
Rg	$7s_{1/2}$	$6d_{5/2}$	$6d_{3/2}$
rel. [a]	-8.415	-5.586	-8.437
nonrel. [a]	-4.301	-10.677	-10.677
nonrel. [b]	-3.300	-7.995	-7.995

[a] the configuration $[Rn]6d^9 7s^2$
[b] the configuration $[Rn]6d^{10}7s^1$

atomic grid points as seen in Table 5.2. Otherwise one spoils the molecular integrations too much. The improved accuracy turns out to be essential also for the Morse-potential fit: the vibrational frequency in Au_2 changes by $+3\,cm^{-1}$, the R_e by $+0.01$ a.u. as compared to the 999 points, and the fit quality χ^2 by almost an order of magnitude. It also shows in Table 5.2 the converge behavior with possible numerical instability. This may come from the irregular oscillation around the true atomic solution and the big error of extrapolation out of the first point near point nuclei.

5.8.3   Basis Construction in Literature

The advantage of using numerical atomic orbitals as basis functions is that one could effectively achieve high accuracy with a small number of basis functions within the DFT scheme and solving the multi-center KS equations. But one has limited flexibility increasing the basis (basis sets from only the solution of neutral, ionized system of same element or other elements [21]). Basis sets as GTO and STO have more freedom, although optimization is need too. In the following is a brief list of the optimization of basis constructions in previous researches with numerical atomic orbitals.

- Varga [50] applied the minimal basis ($1s$ - ns) plus ($np_{1/2}$, $np_{3/2}$, $nd_{3/2}$, $nd_{5/2}$) for coinage metals, ($1s - 6p$) plus ($nd_{3/2}$, $nd_{5/2}$, $nf_{5/2}$, $nf_{7/2}$) for Tl_2 , Pb_2 , Bi_2. And he observes no change by adding ($5f_{5/2}$, $5f_{7/2}$) for the gold dimer. The same choice was taken in his research [56] and Baştuğ's work [19]

- The comment by Liu [37] to Varga's work [50] found better results with an enlarged

Table 5.2: Total energy (Slater functional) for Au_2 calculated at $R = 4.7$ a.u. (minimal basis set and monopole fitting for Hartree energy) with different AO bases, which are with different numbers of atomic grid points N_{atom}. The molecular integration rule is Baerends type with parameters 11/11/11 [19, 55], the matching condition in atomic calculation is 1.0×10^{-9}.

N_{atom}	Molecular Total Energy
100	-38462.11302
300	-38093.3454864
500	-38093.3426193
700	-38093.3456404
900	-38093.3453108
999	-38093.3452478
1100	-38093.3454601
1300	-38093.3454314
1500	-38093.3455485
1700	-38093.3455497
1900	-38093.3455405

basis set in calculations of the gold dimer. His basis set is minimal NAO combined with DZ-STFs for each spinor of $5d$, $6s$, $6p$, $6d$, and a set of $5f$.

- The work [21] of Anton used the minimal basis plus $(6p_{1/2}, 6p_{3/2})$, $(5f_{5/2}, 5f_{7/2})$, $(5g_{7/2}, 5g_{9/2})$, $(6d_{3/2}, 6d_{5/2})$, $(6f_{5/2}, 6f_{7/2})$, and claimed the next additional basis will change the total molecular energy less than 0.01 eV (about 0.00037 a.u.). He achieved highly accurate results for the dimer Pt_2 with an improved model, taking the magnetism into account.

- In Wang's Benchmark calculations [23] even larger basis sets were investigated, which are single-ζ(eg. NAO), plus double-ζ, triple-ζ, Quadruple-ζ for $(n-1)$ and n shells valence $(n-1)d$, ns and np shells , and with further four f and g functions. The conclusion says that up to g state is necessary for highly accurate calculations. All the STFs are optimized in the molecular calculations, rather than in atomic calculations.

Concerning the angular momentum quantum numbers in the multipole expansion of the model density, all of researches [50, 37, 21, 23] confirm that it is sufficient to use the contributions up to the quadrupole terms in the model density.

Table 5.3: Basis set optimization, their spectroscopic constants and effect of changes, in bond length(R_e in a.u.), dissociation energy(D_e in eV), and vibrational frequency(ω_e in cm^{-1}) of Au$_2$, with RLDA density functional

basis sets	R_e	effect(pm)	D_e	effect	ω_e	effect
minimal	4.8142		2.41567		171.56	
+6p	4.7379	4.03762	2.68561	0.269940	186.94	15.38
+6p6d	4.7276	0.54505	2.70400	0.018395	186.27	-0.67
+6p6d7s	4.6977	1.58224	2.81690	0.112901	192.59	6.32
+6p6d7s5f	4.6539	2.31780	2.93905	0.122153	194.97	2.38
+6p6d7s5f5g	4.6286	1.33882	2.99590	0.056845	196.49	1.52
+6p6d7s5f5g7p	4.6261	0.13229	3.00912	0.013225	196.77	0.28
+6p6d7s5f5g7p6h	4.6215	0.24342	3.01813	0.009007	196.79	0.02
+6p6d7s5f5g7p6h8s	4.6210	0.02646	3.02110	0.002966	196.83	0.04
+6p6d7s5f5g7p6h8s7d	4.6204	0.03175	3.02382	0.002721	196.42	-0.41
FEM [24]	4.622		3.018		196.4	

5.8.4   Optimization of Basis

The basis sets optimization for the dimer of the group 11(Ib) of the periodic system are shown in Table 5.3, 5.5, 5.7. The dissociation energies D_e, the bond lengths R_e and the vibrational frequencies ω_e are given to show the improvement and convergence with increasing different type of basis functions. The effect of different basis sets will be compared to the previous work of Varga, Sarpe-Tudoran, and the benchmark of Wang. The work of Wang use also numerical atomic orbitals (NAOs) and kinetically balanced Slater type basis within a four-component relativistic calculation (so called Beijing Density Functional package (BDF)). The relevance of different sort of basis functions for different elements are shown.

To calculate the dissociation energy of molecules, the constituent atomic energy is subtracted. As spin unpolarized calculations are performed presently, the polarization effect (from the open shell atoms) is added from elsewhere, Engel [57] and the paper of Varga [56]. A point nucleus is used in the present calculations. Several digits are provided only for clear comparison, rather than for precision. The benchmark calculations of FEM utilizes seventh order FEM polynomials with a coordinate transformation of type $\nu = 3$ [24] and spatial extension of FEM $D = 30$. For more details see paper [17].

5.8.5 Basis sets of Au$_2$

The molecule Au$_2$ is taken as a standard system for the research of relativistic calculations, therefore many details could be found in the literature. It is first compared here. Later we investigate the light element Ag$_2$ and the super-heavy Rg$_2$.

Table 5.4: Comparison between the effects of $5f$, $5g$, $6h$ in the present work and f-, g-, h-type functions of Wang [23] , with RLDA and LDA, respectively, in Au$_2$

function	δ R$_e$ [a]	δ R$_e$ [23]	δ D$_e$ [a]	δ D$_e$ [23]	δ ω_e [a]	δ ω_e [23]
$5f$	-2.31780 pm	-2.27 pm	0.122153 eV	0.1197 eV	2.38 cm^{-1}	2.16 cm^{-1}
$5g$	-1.33882 pm	-0.87 pm	0.056845 eV	0.0447 eV	1.52 cm^{-1}	1.32 cm^{-1}
$6h$	-0.24342 pm	-0.08 pm	0.009007 eV	0.0048 eV	0.02 cm^{-1}	0.14 cm^{-1}

[a] present work

- The earlier four-component DFT calculations of Varga [56] show the dissociation energy of Au$_2$ 3.34 eV with spin-polarization effect. The improved result 2.70 eV could be deduced after the important multipole expansion of the Hartree potential in a next paper [50], has an effect 0.64 eV in total energy up to quadrupole. (The shorter bond length and larger vibrational frequency were shown in [56] with monopole calculation, the improved corresponding values for RLDA were not given in the next calculation [50], but only for RGGA). For checking of the statement of Varga with his rather small basis sets (minimal basis plus $6p$ and $6d$), Liu compares in his comment [37] three different basis sets A,B,C, where A, for the purpose of simulating Varga's calculation, consists of NAOs plus a single-zeta STF for $6p$ and $6d$ (the difference is that Varga's $6p$ and $6d$ are from ionized atoms). Liu obtained the following result: (R_e: 4.733 a.u., D_e: 2.679 eV, ω_e: 187 cm^{-1}). The present evaluation with the same type of basis sets confirm them (R_e: 4.7276 a.u., D_e: 2.704 eV, ω_e: 187.3 cm^{-1}).

- s-type basis functions. The missing flexibility in s-type basis functions is commented [37], Varga did not use s-type functions, and Tudoran got it partly in another way. As described in the Tudoran thesis, keeping the $1s$ up to $5p$ core and semi-core basis functions from neutral atom, the $5d$ and $6s$ valence functions are obtained from atoms with ionization degree +0.29 . One could take this option as an extra freedom for $5d$ and $6s$. This causes a 0.0263 eV deeper molecular energy in her calculation. With $6p$ (+2.5 degree ionization) and $5f$ (+4.5 degree ionization) she has shorter bond length (4.67 a.u.) and deeper energy (3.15 eV). The comparison to

another basis set construction, $5d$ and $6s$ from neutral atom with $6p$, $5f$ (+4.0 degree ionization for both might not be the optimal), shows a difference (contribution from the extra freedom of $6s$ and $5d$) of 0.03 a.u. in bond length, and 0.08 eV in RLDA. The effect found in the present works from $7s$, $8s$ and $6d$, summed up, is 0.04 a.u. in bound length and 0.134 eV in energy. Therefore, additional s-type functions have more effect than $5d$ and $6s$ from ionized atoms. No more basis is added by Tudoran for the limitation of the computer memory in cluster calculations. But it is important to mention that $7s$ is not added too in the paper of Anton [39], although very good agreement is achieved to the experimental value for Pt_2 with the extension of the relativistic density functional theory to the non-collinear form. Effect of missing s-type basis function needs to be clarified.

- f-type basis used by Tudoran gives an effect of about 0.1 eV in binding energy. In the present calculation the effect of 0.122 eV agrees with it. Summing the R_e 4.7379 a.u. (of minimal basis with $6p$) and the effect of $5f$ (-0.0438 a.u.), one obtains 4.6941 a.u., which is close to the result of Tudoran 4.70 a.u..

  A comparison of the effect from $5f$, together with effects of $5g$ and $6h$, to Wang's work [23] is shown in Table 5.4. Two results agree quite well except the $6h$ effect of Wang is smaller, they estimated it by scalar relativistic ZORA (zero order regular approximation) results [23].

- Generally the main contribution 80% is from minimal basis set, and as Wang [23] said they serve as the backbone. Then quite large effects come from $6p$, $5f$, $7s$, $5g$ (descending in the absolute contribution on energy and length, see in Table 5.3). One should not miss one of them for a good description of these properties. Further s-, p-, d-type functions ($8s$, $7p$, $7d$) give small effects of 2.7%, 4.8%, 14.7% of the $7s$, $6p$, $6d$ in total energy, respectively. $6h$ is needed, when one requires an accuracy within 10 meV.

5.8.6 Basis sets of Ag_2

Ag_2, as a light counterpart, is quite often compared to Au_2, to show that Au_2 has more relativistic effect. The valence atomic orbitals of Au_2 contract $6s$ in size more than $5s$ of Ag_2 and expand $5d$ more than $4d$ of Ag_2. Therefore, in Ag_2, $4d$ functions take a smaller share in the binding than $5d$ in Au_2.

- the main contribution 81.8% are from minimal basis, and $5p$, $6s$, $4f$ gives large effects. The percentage in total binding energy of $5p$, $6s$ (9.3%, 3.9%) is larger than the corresponding functions $6p$, $7s$ (8.9%, 3.7%) of Au_2, in contrast to the smaller

Table 5.5: Basis set optimization, their spectroscopic constants and effect of changes, in bond length(R_e in a.u.), dissociation energy(D_e in eV), and vibrational frequency(ω_e in cm^{-1}) of Ag$_2$, with Slater density functional

basis set	R_e	effect(pm)	D_e	effect(eV)	ω_e	effect
minimal	4.8875		1.53735		178.33	
+5p	4.7952	-4.88	1.71151	0.17416	191.77	13.44
+5p5d	4.7898	-0.29	1.71698	0.00547	193.12	1.35
+5p5d6s	4.7677	-1.17	1.78985	0.07287	198.34	5.22
+5p5d6s4f	4.7336	-1.80	1.85254	0.06269	198.95	0.61
+5p5d6s4f6p	4.7320	-0.08	1.85518	0.00264	199.24	0.29
+5p5d6s4f6p5g	4.7169	-0.80	1.87314	0.01796	199.77	0.53
+5p5d6s4f6p5g6d	4.7157	-0.06	1.87532	0.00218	199.24	-0.53
+5p5d6s4f6p5g6d6h	4.7134	-0.12	1.87655	0.00123	199.27	0.03
+5p5d6s4f6p5g6d6h7p	4.7128	-0.03	1.87799	0.00144	199.49	0.22
FEM [24]	4.712		1.8855		200.3	

percentage of $4f$ (3.3%) of Ag$_2$ than $5f$ (4.0%) of Au$_2$. The $5g$ contribution is already quite small, contributing in energy about a quarter as the $5g$ in Au$_2$, even though it is still larger than from the other functions $5d$, $6p$, $7p$, $6h$ of Ag$_2$. All these show the smaller importance of high angular momentum in Ag$_2$ binding.

- confirmation of effects from f-, g-, h-type basis (see Table 5.6). The present values (Slater functional) agree in magnitude to Wang's (RLDA) [23].

5.8.7 Basis sets of Rg$_2$

Rg$_2$ is quite different to Ag$_2$ and Au$_2$ in the basis construction.

- the contributions of $7s$ and $6d$ in the minimal basis is small

- $7p$ gives a large effect in binding energy, and shorten the distance by 38 pm

- with a similar distance as Ag$_2$, $6f$ gives much more effect than $4f$ of Ag$_2$ (0.2069 eV vs 0.06269 eV), $5g$ (0.09448 eV vs 0.01796 eV), $6h$ (0.016137 eV vs 0.00123 eV).

- functions, such as i-type with even higher angular momentum might not be neglected for this system. For practical limitation it is not investigated.

Table 5.6: Comparison between the effects of $4f$, $5g$, $6h$ in the present work and f-, g-, h-type functions of Wang [23] , with Slater and LDA, respectively, in Ag_2

function	δR_e [a]	δR_e [23]	δD_e [a]	δD_e [23]	$\delta \omega_e$ [a]	$\delta \omega_e$ [23]
$4f$	-1.80 pm	-1.29 pm	0.06269 eV	0.0559 eV	0.61 cm^{-1}	0.22 cm^{-1}
$5g$	-0.80 pm	-0.54 pm	0.01796 eV	0.0139 eV	0.53 cm^{-1}	0.74 cm^{-1}
$6h$	-0.12 pm	-0.08 pm	0.00123 eV	0.0022 eV	0.03 cm^{-1}	0.13 cm^{-1}

[a] present work

Table 5.7: Basis set optimization, their spectroscopic constants and effect of changes in bond length(R_e in a.u.), dissociation energy(D_e in eV) and vibrational frequency(ω_e in cm^{-1}) of Rg_2, with Slater density functional

basis sets	R_e	effect(pm)	D_e	effect(eV)	ω_e	effect
minimal	5.8108		0.139952		70.50	
+7p	5.0912	38.0796	0.933201	0.793247	130.25	59.75
+7p7d	5.0674	1.25944	0.953231	0.0200278	131.42	1.17
+7p7d8s	4.9953	3.81537	1.10349	0.150263	135.96	4.54
+7p7d8s8p	4.9536	2.20667	1.15443	0.0509402	143.09	7.13
+7p7d8s8p6f	4.8120	7.49315	1.36135	0.206917	159.50	16.41
+7p7d8s8p6f5g	4.7561	2.9581	1.45583	0.0944788	165.88	6.38
+7p7d8s8p6f5g6h	4.7465	0.50801	1.47196	0.0161365	175.52	9.64
FEM	4.7343		1.5085		160.40	

These confirm the main character of d-type binding in Rg_2.

The Table 5.7 also shows that the ω_e of Rg_2 seems not to converge to the FEM value. It could be a problem of too low multipoles in the Hartree potential which would mean too little electronic Coulomb repulsion, but it also could mean that LCAO converges to another molecular state than FEM, but energetically close to it. This is not decided yet even though the other quantities like R_e and D_e seem to converge against the FEM values and therefore might suggest that LCAO converges to the same state. Too little Coulomb repulsion would make the molecular state energetically too deep, but there is no clear indication for this. But it could be a real effect that another molecular excited state might be very close in R_e and D_e yet with a bigger ω_e. Such an assumption also makes a lot of sense since the groundstate (lowest energy molecular state) has the lowest ω_e of nearby excited states which could be rather close in Rg_2 since it does not have the same

s-binding as Ag_2 and Au_2, but d contributions dominant in the groundstate and s-binding in a low excited state, making this excited state in its properties closer to Ag_2 and Au_2 which would mean ω_e closer to Au_2.

5.8.8 Accuracy

Table 5.8: Spectroscopic constants, bond length (R_e in a.u.), dissociation energy (D_e in eV), and vibrational frequency (ω_e in cm^{-1}) of Ag_2, with different density functionals and methods

Ag2	method	R_e	D_e	ω_e
Slater	4-sp LCAO	4.7128	1.87799	199.49
Slater	TVDB LCAO	4.7128	1.87796	199.48
Slater	FEM minimax	4.712	1.8855	200.3
RLDA	4-sp LCAO	4.6909	2.284992	206.24
RLDA	TVDB LCAO	4.6909	2.284995	206.24
RLDA	FEM minimax	4.689	2.2895	206
RGGA	4-sp LCAO	4.8381	1.75089	186.37
GGA	BDF [23]	4.830	1.735	182.3
	Exp. [54]	4.79	1.65	192.5

The spectroscopic constants of Ag_2, Au_2, Rg_2 with three density functionals are documented and discussed in the Tables 5.8, 5.9, 5.10 to show the accuracy achieved. Followed later is the comparison of the four-spinor and the TVDB method.

The results of Ag_2 in Table 5.8 are all satisfactory for the three density functionals. The agreement to the Benchmark values demonstrates the basis set is large enough to reach small truncation errors and to make safe judgments on the functionals. The errors are with Slater functional (R_e: 0.001 a.u. (0.05pm), D_e: 0.0075 eV, ω_e: 1 cm^{-1}), and with RLDA (R_e: 0.002 a.u. (0.10pm), D_e: 0.0045 eV, ω_e: 0.2 cm^{-1}), and with RGGA (R_e: 0.008 a.u. (0.53pm), D_e: 0.016 eV, ω_e: 4 cm^{-1}), while the functional errors (between the approximate functionals and experimental values) are about one order of magnitude bigger in R_e (Slater 0.078 a.u., RLDA 0.101 a.u., RGGA 0.040 a.u. (factor 5)), and in D_e (Slater 0.24 eV, RLDA 0.64 eV, RGGA 0.09 eV (factor 5)). It is a safe statement, for instance, that all the three functionals have deeper dissociation energies than the experiment.

The calculation of Au_2 with RLDA is successful too (see Table 5.9). The truncation error 0.002 a.u. in R_e (compared to a functional error of 0.05 a.u.), 0.006 eV in D_e (compared

Table 5.9: Spectroscopic constants, bond length(R_e in a.u.), dissociation energy(D_e in eV), and vibrational frequency(ω_e in cm^{-1}) of Au$_2$, with different density functionals and methods

Au$_2$	method	R_e	D_e	ω_e
Slater	4-sp LCAO	4.6361	2.7030	181.7
Slater	TVDB LCAO	4.6364	2.7030	181.6
Slater	FEM minimax	4.629	2.712	193.5
RLDA	4-sp LCAO	4.6204	3.0238	196.4
RLDA	TVDB LCAO	4.6204	3.0237	196.4
RLDA	FEM minimax	4.622	3.018	196.4
RGGA	4-sp LCAO	4.7612	2.235	180.8
GGA	BDF [23]	4.724	2.376	179.1
	CCSD(T) [53]	4.702	2.19	187
	Exp. [54]	4.67	2.344	190.9

to 0.674 eV), respectively. The R_e, 0.002 a.u. shorter than the Benchmark, suggests the missing of a high angular momentum expansion in the Hartree potential. Slater functional values are also very good in R_e and D_e, with truncation error 0.008 a.u. and 0.009 eV, respectively. The large errors, unfortunately, of ω_e in Slater calculation, as well as R_e and D_e in RGGA (R_e (0.037 a.u.) factor 4 and D_e (0.141 eV) factor 9 larger than the Ag$_2$ error with RGGA) mean that the optimization and/or basis size is not as good any more. This large difference within RGGA can't be explained by relativistic corrections to the density functional, which could be estimated to be about 0.01 a.u. in R$_e$, 0.033 eV in D$_e$, and 1.5 cm^{-1} in ω_e by the difference between NLDA and RLDA in the work [24]. A list of the progress in Liu's calculations, (in 1999 [58], 4.7489 a.u., 2.22 eV, 183 cm^{-1}), (in 2000 [37], 4.749 a.u., 2.33 eV, 183 cm^{-1}), and (in 2005 [23] in my Table 5.9) gives a hint of the inefficiency of present RGGA basis sets. Therefore the basis sets with ionization degree from RLDA optimization are not suitable for RGGA calculations. One needs basis set optimization for RGGA itself. While TVDB RGGA calculation is not finished yet, the four-spinor RGGA value is only documented here to show the phenomena. The best work of the coupled cluster method [53], whose achievement is within 1 pm in R_e, 0.1 eV in D_e (0.15 eV for the new experimental value), and a few wave numbers in ω_e, is listed in the Table 5.9 too (1 kcal/mol taken as chemical accuracy).

For Rg$_2$ the LCAO values in Table 5.10 are moderately good, 0.012 a.u. difference in R_e, 0.04 eV and 0.06 eV in D_e with Slater and RLDA functionals respectively. RGGA value of Rg$_2$ has no benchmark yet. Literature shows only the result of Liu in 1999 [58],

Table 5.10: Spectroscopic constants, bond length (R_e in a.u.), dissociation energy (D_e in eV), and vibrational frequency (ω_e in cm^{-1}) of Rg$_2$, with different density functionals and methods

Rg2	method	R_e	D_e	ω_e
Slater	4-sp LCAO	4.7465	1.4720	175.5
Slater	TVDB LCAO	4.7467	1.4719	175.6
Slater	FEM minimax	4.7343	1.5085	160.40
RLDA	4-sp LCAO	4.7508	1.7186	153.7
RLDA	TVDB LCAO	4.7508	1.7185	153.7
RLDA	FEM minimax	4.7388	1.6556	161.93
RGGA	4-sp LCAO	4.9001	1.41653 [a]	137.4
GGA	BDF [58]	4.9133	0.88 [b]	137

[a] nonspin-polarization result
[b] basis set up to f-type function

with basis functions only up to f-type , without g- and h-type functions. If one adds the contribution of them (taking the present calculation, for example), the value of Liu(1999) will be about 0.12 eV larger, leading to a D_e value 1.00 eV (from 0.88 eV). The spin polarization of the atomic calculation is not available yet. An estimate could be between 0.24 eV (from NLDA) and 0.32 eV (from Slater); let's take 0.26 eV (as in Ag$_2$ and Au$_2$ the spin polarization of RGGA is slightly bigger than RLDA). Subtracting this gives 1.16 eV, which is still different to the value 1.00 eV. Again the e-e relativistic correction [24] (0.0188 a.u. in R_e, 0.041 eV in D_e) can't explain the possible difference 0.16 eV. According to the larger contribution of g- and h-type functions in Rg$_2$, a multipole expansion of the Hartree potential beyond quadrupole is needed. The additional basis of s-, p-, d-type contributes less than in the case of Ag$_2$ and Au$_2$, thus the fitting of dipole and quadrupole is not as sufficient as for the other two molecules. These two reasons could lead to a deeper total molecular energy by this amount.

In general, the present work has good results, especially in Ag$_2$ and Au$_2$ within the local functionals, where I optimized the corresponding basis sets. The last, but not least, important comparison is between traditional four-spinor and TVDB methods, to check if it is less than the truncation error, say 0.01 eV, and to which accuracy they differ.

5.8.9 Comparison of the two methods

One observes that the difference is small between four-spinor LCAO and TVDB LCAO within two local density functionals, Slater and RLDA (see Table 5.11). The difference

Table 5.11: Comparison of four-spinor LCAO and TVDB LCAO on Ag_2, Au_2, Rg_2, average energy difference (in a.u.) of 11 points in interval $\Delta = 0.2$ a.u. and ratio of value between two end points

functional	Ag_2		Au_2		Rg_2	
	average	ratio	average	ratio	average	ratio
Slater	4.73×10^{-7}	1.22	2.05×10^{-6}	1.47	4.61×10^{-6}	1.46
RLDA	4.64×10^{-7}	1.50	2.04×10^{-6}	1.50	4.42×10^{-6}	1.47

comes from the improvement of the small components of the molecular orbitals and the additional projection power against contamination. The molecular potential, instead of atomic potential, in the denominator of the small component in basis functions, and the additional balanced basis functions describes more correctly the small components of molecular orbitals and should give better results. The additional balanced basis functions serve also to prevent from phenomena such as variational collapse and contamination, discretizing the negative continuum.

The present calculation shows differences of about 10^{-6} a.u.. The improvement by the TVDB method is so small, compared to the binding energy, that it illustrates the four-spinor LCAO to be still safe in chemistry calculation. The demonstration of the improvement of TVDB in a well behaved way for all inter-nuclear distance shows the variational safety, too. It is found the increasing trend of improvement with large nuclear charge Z. This is attributed to all occupied single particle functions, which all have improved small components. Another fact is that the improvement at the smaller inter-atom distance is about 1.5 bigger than at the larger inter-atom distance, when the two distances are taken around bond distance in an interval 0.20 a.u., for instance, 4.52 a.u. and 4.72 a.u. in Au_2 with RLDA. The larger improvement by molecular potentials from atomic potentials for shorter internuclear distance is reasonable. And one could expect an even larger change at very small internuclear distances, such as scattering problems in Chapter 3 and the next chapter. Even worse is that serious contamination or collapse might not be avoided any longer with the traditional method.

Chapter 6

Many-Electron Spectrum of Quasi-Molecules

The four-spinor LCAO method was also applied in relativistic many-electron correlation diagrams calculations [59, 18, 25, 26, 27, 28, 29] to get the energy eigenvalues and eigenfunctions as a function of the internuclear distance R for dynamic research purposes. These eigenfunctions are a good base for time-dependent equations in adiabatic heavy ion collisions.

The work [59] was the first for relativistic many-electron SCF correlation diagrams for an improved (better than a nonrelativistic estimate) understanding of the collision from the one-electron correlation diagrams (a research before more correct many-electron correlation diagrams). In paper [18] differential elastic scattering cross sections for Ne-Ne were calculated and agreed well with experimental values to test the quality of the quasi-molecular potential. And time-dependent many-electron coupled-channel calculations were performed in [25]. The investigation there was the K-L-vacancy-sharing process of Ar^{4+} and Ar^{12+} ions on Ca solid targets. Schulze and Anton [26, 28, 27, 29] investigated molecular-orbital x-rays in Cl^{16+}-Ar collisions and U^{92+}-Pb collisions.

In short, the many-electron SCF correlation diagrams are only to generate basis functions for time-dependent many-electron coupled-channel calculations. The correlation diagrams themselves are solved with atomic basis sets in LCAO SCF calculations.

For the light system Ne-Ne ($R \leq 0.7$ a.u.) in [18] the basis sets complement the minimum basis set with additional wave functions ($1s_{1/2}$ to $4s_{1/2}$), which are from atomic calculations in the monopole potential of the two nuclei at the center of the two nuclear charges (as described in Chapter 3).

For the heavy system Pb-Pb with 96 electrons [59], a very large number of numerical DFS atomic basis functions of lead and additionally those of the united atom are utilized.

In those calculation, a pre-orthogonalization was done before the derivation of the eigen-

value equations. It states [59] that to avoid spurious states the pre-orthogonalization is absolutely necessary so that linear dependence would be removed. And one notes that the numerical accuracy is only in the order of 10^{-6}.

What does lead to the spurious states in these kind of calculation? Linear dependence or the property of the Dirac Hamiltonian itself? That is why I do the comparison here. It is clear that linear dependent basis sets produce a large error enhancement. But my research will show that the TVDB method could achieve the correct spectrum when traditional LCAO four-spinor method fails with the same (good) numerical accuracy (in the order of 10^{-8})

We perform DFS calculation for two quasi-molecular multi-electron systems, both Ne-Ne and Pb-Pb with only 20 electrons, with the TVDB method and the traditional LCAO four-spinor method. The basis constructions are the same for comparison purposes. And the basis sets are constructed including the modified monopole potential contributions from the other center(s). The only difference is the nuclear charge, light and heavy.

Table 6.1: the total energy, the energy contributions, and the low-lying states of 20-electron Ne-Ne quasi-molecule at internuclear distance $R = 0.02$ a.u. with 2- and 3-center basis sets ; basis of every center is from $1s_{1/2}$ to $3p_{3/2}$, $4s_{1/2}$; all in atomic units; the error for integral is less than $.9238 \times 10^{-8}$; the energies of the atomic orbitals are listed in the last two columns.

J_z	4-SP 2-c basis	4-SP 3-c basis	TVDB 2-c basis	TVDB 3-c basis	middle basis	left, right basis
1/2	-138.1779	-138.1995	-138.1779	-138.1990	-140.5470	-137.3225
1/2	-14.64962	-14.65451	-14.64962	-14.65445	-14.84917	-14.59088
1/2	-12.56030	-12.54886	-12.56032	-12.54877	-12.45584	-12.49996
1/2	-12.34507	-12.33138	-12.34511	-12.33132	-12.32071	-12.36546
3/2	-12.27758	-12.26375	-12.27762	-12.26370	-12.32071	-12.36546
1/2	-1.632246	-1.634184	-1.632245	-1.634194	-1.655635	-1.626166
1/2	-1.035669	-1.036481	-1.035669	-1.036488	-1.022437	-1.031362
1/2	-1.013361	-1.013022	-1.013363	-1.013034	-1.008127	-1.017104
3/2	-1.006276	-1.005804	-1.006279	-1.005817	-1.008127	-1.017104
1/2	-.1145657	-.1142282	-.1145656	-.1142277	-.1161466	-.1151822
$\sum_i \epsilon_i$	-389.6252	-389.6034	-389.6253	-389.6020	-394.6077	-387.9025
E_{total}^{DFS} †	-662.5863	-662.9397	-662.5855	-662.9387	-668.4373	-660.7901

† the repulsion energy between two nuclei -5000 a.u. is subtracted.

Table 6.1 shows the results of 2-center and 3-center basis sets for Ne-Ne with the two methods. Obviously with the light element Ne and the basis set ($1s_{1/2}$ to $4s_{1/2}$) there are

no spurious states. And it is fairly clear that the results of both four-spinor LCAO and TVDB are close to each other at least up to the fifth digit after the decimal point with a 2-center basis set for every molecular eigen-states. With a 3-center basis set nearly the same quality is achieved with only exception of the lowest state, which has one less digit of agreement. The total energies differ in the third or fourth digit after the decimal point. The 3-center basis set leads to a deeper total energy than the 2-center basis set, showing the convergence. The AO basis eigen-energies (left, right and middle) are also shown in the table. Because the monopole potential contribution of the other nucleus is included, the basis sets have a similar structure as the molecular spectrum at short distances. The linear dependence does not show up within this basis size.

Table 6.2: the total energy, the energy contributions, and the low-lying states of 20-electron Pb-Pb quasi-molecule at internuclear distance $R = 0.02$ a.u. with 2- and 3-center basis sets; basis of every center is from $1s_{1/2}$ to $3p_{3/2}$, $4s_{1/2}$; all in atomic units; the error for integral is less than $.713 \times 10^{-8}$; the energies of the atomic orbitals are listed in the last two columns.

J_z	4-SP 2-c basis	4-SP 3-c basis	TVDB 2-c basis	TVDB 3-c basis	Atom shell	middel basis	left, right basis
1/2		-17212.8**					
1/2	-15952.5**	-12028.5**					
1/2	-7782.358	-7648.780	-7775.843	-7844.063	$1s_{1/2}$	-8138.663	-8030.104
1/2	-4702.585	-4655.860	-4719.403	-4731.381	$2s_{1/2}$	-2579.902	-2766.517
1/2	-2948.997	-2932.746	-2952.941	-2974.030	$2p_{1/2}$	-3960.836	-3537.435
3/2	-2622.419	-2612.367	-2627.955	-2645.593	$2p_{3/2}$	-3292.876	-2950.989
1/2	-2459.709	-2454.216	-2464.390	-2487.929			
1/2	-1701.012	-1697.846	-1709.425	-1714.597	$3s_{1/2}$	-1191.432	-1263.902
1/2	-1440.178	-1436.397	-1414.760	-1425.219	$3p_{1/2}$	-1537.815	-1462.623
1/2	-1291.840	-1295.023	-1294.877	-1307.445	$3p_{3/2}$	-1407.417	-1305.609
1/2	-1253.951	-1250.238	-1246.483	-1256.049			
3/2	-1250.785	-1246.511	-1246.397	-1245.174	$4s_{1/2}$	-674.240	-706.672
3/2	-1193.764	-1202.859	-1196.405	-1212.807			
1/2	-1138.179	-1146.197	-1139.527	-1155.437			
$\sum_i \epsilon_i$	-84311.0	-107949.1	-54904.9	-55263.0		-54967.0	-52560.9
E_{total}^{DFS} †	-89678.1	-114003.7	-60194.4	-60444.5		-58638.2	-56133.1

† the repulsion energy between two nuclei -336200 a.u. is subtracted;
** means spurious states.

Table 6.2 shows the results of the 2-center and 3-center basis sets for the system Pb-Pb. Therefore it is expected that the similar quasi-molecular system Pb-Pb, with the same

construction of the basis as Ne-Ne, has not large linear dependence problems (even smaller because relativistic effects cause contraction of s- and p- type levels of the basis sets and thus diminish the left-right overlap).

If any spurious states show up, this should be the variational collapse problem for the only difference of the heavier nuclear charge. As shown in table 6.2 one spurious state appears below the true spectrum with the 2-center basis set with the four-spinor LCAO method, and one state more with the 3-center basis set. (The spurious states come out already from the very beginning of the SCF calculation, rather than later in the iteration process.) Sum of the eigenvalues and the total energy are quite different between the two methods with the same basis set because of the contamination by the negative continuum. Spurious states do not show up in the TVDB method. Atomic basis energies are listed in the last two columns too, showing large relativistic effects especially in $1s_{1/2}$ and $2p_{1/2}$, which correspond to $1(1/2)_g$ and $1(1/2)_u$ in the quasi-molecule.

Table 6.3 has the calculation with an enlarged basis, basis size of every center from ($1s_{1/2}$ to $4s_{1/2}$) increasing to ($1s_{1/2}$ to $4f_{7/2}$), which is larger than or equal to ref. [26, 28, 27, 29]. More spurious states appear below or in the spectrum with the four-spinor LCAO method, while the TVDB method works still quite well. The TVDB total energy shows convergence of the total energy with increasing basis either from 2-center to 3-center or from ($1s_{1/2}$ to $4s_{1/2}$) basis to ($1s_{1/2}$ to $4f_{7/2}$) basis (comparing table 6.2 and table 6.3).

In the calculations [18, 59] the pre-orthogonalization helps to remedy linear dependence problems and partly to reduce the severity of the variational problem, but there is no proof that a linear independent basis has no variational collapse. The two cases here show the failure of traditional four-spinor calculations without pre-orthogonalization, and the success of the TVDB LCAO method. With the same basis size (in large component) in these cases the TVDB method gets reasonable results without pre-orthogonalization. This fact demonstrates that linear dependence is not serious in these calculation, and the variational collapse can be avoided with the TVDB method.

Table 6.3: the total energy, the energy contributions, and the low-lying states of 20-electron Pb-Pb quasi-molecule at internuclear distance $R = 0.02$ a.u. with 2- and 3-center basis sets; basis of every center is from $1s_{1/2}$ to $4f_{7/2}$; all in atomic units; the error for integral is less than $.713 \times 10^{-8}$; the energies of the atomic orbitals are listed in the last two columns.

J_z	4-SP 2-c basis	4-SP 3-c basis	TVDB 2-c basis	TVDB 3-c basis	Atom shell	middle basis	left, right basis
		-47179.9**					
		-29324.6**					
	-30969.1**	-16969.5**					
	-9081.0**	-9921.9**					
1/2	-7849.979	-8043.416	-7832.949	-7953.728	$1s_{1/2}$	-8138.663	-8030.104
1/2	-4783.755	-4964.506	-4760.884	-4818.339	$2s_{1/2}$	-2579.902	-2766.517
	-3483.9**						
	-3342.1**	-4629.9**					
					$2p_{1/2}$	-3960.836	-3537.435
					$2p_{3/2}$	-3292.876	-2950.989
1/2	-3002.028	-3076.387	-2986.545	-3017.718	$3s_{1/2}$	-1191.432	-1263.902
3/2	-2666.403	-2709.535	-2654.528	-2669.845	$3p_{1/2}$	-1537.815	-1462.623
1/2	-2479.339	-2513.810	-2486.266	-2498.269	$3p_{3/2}$	-1407.417	-1305.609
		-2042.5**					
1/2	-1719.297	-1647.853	-1718.414	-1714.744	$3d_{3/2}$	-1418.684	-1382.187
1/2	-1451.168	-1456.838	-1451.808	-1447.642	$3d_{5/2}$	-1282.050	-1273.053
1/2	-1305.605	-1277.012	-1307.708	-1313.322	$4s_{1/2}$	-674.240	-706.672
3/2	-1300.408	-1271.741	-1301.235	-1294.085	$4p_{1/2}$	-809.537	-783.876
1/2	-1278.024	-1251.395	-1279.306	-1270.237	$4p_{3/2}$	-763.114	-721.693
3/2	-1229.505	-1190.882	-1231.211	-1223.652	$4d_{3/2}$	-772.241	-752.228
3/2	-1207.950	-1183.470	-1210.496	-1215.119	$4d_{5/2}$	-715.405	-709.230
5/2	-1189.755	-1145.193	-1192.066	-1184.956	$4f_{5/2}$	-698.822	-698.885
1/2	-1141.917	-1139.122	-1146.870	-1155.820	$4f_{7/2}$	-679.135	-679.281
$\sum_i \epsilon_i$	-138753.6	-168392.1	-55559.3	-55995.9		-54967.0	-52560.9
E_{total}^{DFS} †	-143485.1	-173538.1	-60466.5	-60717.4		-58638.2	-56133.1

† the repulsion energy between two nuclei -336200 a.u. is subtracted;

** means spurious states.

Chapter 7

Conclusion and Outlook

The present research starts searching for the correct eigenstate spectrum of the relativistic one-electron systems H_2^+ and Th_2^{179+}, comparing the two-component spinor minimax LCAO and the traditional four-spinor LCAO method. Although the two-spinor minimax LCAO method is quite time consuming to construct the H matrix and perform a full diagonalization in every iteration for E^{MO} in the denominator of the minimax formula (equation 3.3), it is bounded from below, yielding the whole spectrum of the molecules (both light and super-heavy molecules) correctly. But the traditional four-spinor LCAO could not project well against the negative continuum in the super-heavy quasi-molecular calculation, with the presence of spurious and contaminated states in the spectrum. Two-spinor minimax LCAO provides reliable information on the complete spectrum of the relativistic Th_2^{179+}; two-spinor minimax FEM (or other basis sets) may then be used to obtain more precise energies.

The investigation proceeded to the kinetic balance method and new linear balance basis methods on the same super-heavy quasi-molecular system, in order to avoid consuming too much time in the iterative procedure for E^{MO} in the denominator of the minimax energy functional. The TVDB LCAO method is in very good agreement with the minimax LCAO, while other methods, TVB, KB and traditional LCAO may be much worse. The small difference between TVDB and minimax LCAO is attributed to their similar projection power against the negative continuum. Therefore TVDB Defect Balance is the most promising method, among all methods compared here, as it defines a linear eigenvalue approach in contrast to the non-linear Minimax LCAO process, and with the very good projection quality even for super-heavy systems. And it is worth noting that the molecular potential in the denominator is crucial for good projection, rather than the energy dependence.

In order to demonstrate the projection behavior of the TVDB method in multi-electron systems, first we applied it to the chemical systems, Ag_2, Au_2 and Rg_2, around equilibrium

distance with the requirement of chemical accuracy, and compared it to traditional 4-spinor LCAO. The difference between the two methods is quite regular and small, being two orders less than the error due to incompleteness of the basis set. Thus one could conclude that within RLDA and Slater density functionals chemistry calculation with both methods are variationally safe, in the sense that the possible deviation of traditional LCAO is less than 0.13 meV even in the dimer of a super-heavy element, and the TVDB method has an improved safety than the other. Since the TVDB method, with the balanced basis set, cost more time in matrix element calculation and solution of the eigenfunctions, the traditional four-spinor LCAO is still favorable in chemistry simulations.

Besides, the success of the basis construction within chemical accuracy demonstrated the flexibility of basis sets in our scheme. The details prove the even more relativistic effect in Rg_2 than Ag_2 and Au_2 and more binding energy from d-type valence orbitals. Obviously higher angular momentum than quadrupole needs to be applied for the Rg_2 Hartree energy calculation. Since the fitting procedure of the density is more expensive with all density basis functions from NAOs and higher angular momentum, it is better to make the core density fixed or projected out to reduce the fitting space. More studies on the converge behavior of fitting a basis set helps for the accuracy of the calculation.

Since the kinetic balance method was not suitable with numerical AOs, it was not compared in the present chemical calculation. As TVDB LCAO is superior over the KB method, it is recommended for checking the variational safety of KB calculations, if no numerical molecular standard is available and the nonlinear minimax principle is too expensive. This suggestion arises partly from the efforts of Gaussian basis optimization for the KB scheme and tests in atomic cases but no detailed investigations on molecular variational safety are available yet.

As suggested by Wang [23], the achievement of accuracy encourages the research of new parameterizations of DFT, especially for systems with heavy and super-heavy atoms to reduce the inherent error in DFT. More studies on different other systems with heavy and super heavy atoms are needed to calibrate DFTs.

Finally a further comparison of the two methods has been made in many-electron quasi-molecular calculations with different basis sizes. For light systems like Ne-Ne at $R = 0.02$ a.u. both the TVDB method and the traditional four-spinor LCAO work well. differing very little. But for super-heavy systems (like Pb-Pb with 20 electrons) the traditional four-spinor LCAO shows spurious states, which is not caused by linear dependence, but by variational collapse. The TVDB method keeps the variational stability and works well when increasing the basis size. It was only a quite simple illustration since the optimization of the basis set was not done. In order to achieve high accuracy and convergence, systematic investigations are needed with the TVDB method, as well as the investigation on the linear dependence. The consideration of QED is important too in that case, but has been left out in the present work.

Bibliography

[1] G. L. Malli, *Relativistic Effects in Atoms, Molecules, and Solids* (Plenum Press, New York, 1983).

[2] G. L. Malli, *Relativistic and Electron Correlation Effects in Molecules and Solids* (Plenum Press, New York, 1994).

[3] R. E. Stanton and S. Havriliak, J. Chem. Phys. **81** (1984) 1910.

[4] W. Kutzelnigg, Chem. Phys. Lett. **25** (1984) 107.

[5] L. Visscher, O. Visser, P.J.C. Aerts, H. Merenga, W.C. Nieuwpoort, Comp. Phys. Comm. **81** (1994) 120.

[6] W. C. Nieuwpoort, P. J. C Aerts, L. Visscher, in *Relativistic and Electron Correlation Effects in Molecules and Solids*, edited by G. L. Malli (Plenum Press, New York, 1994), pp. 313–347.

[7] J. D. Talman, Phys. Rev. Lett. **57** (1986) 1091.

[8] J. Dolbeault, M. J. Esteban. E. Séré and M. Vanbreugel, Phys. Rev. Lett. **85** (2000) 4020.

[9] J. Dolbeault, M. J. Esteban, E. Séré, Calc. Var. **10** (2000) 321.

[10] J. Dolbeault, M. J. Esteban, and E. Séré, J. Func. Anal. **174** (2000) 208.

[11] L. LaJohn, J. D. Talman, Theor. Chem. Acc. **99** (1998) 351.

[12] A. Rosén, D. E. Ellis, J. Chem. Phys. **62** (1975) 3039.

[13] O. Kullie , D. Kolb, A Rutkowski, Chem. Phys. Lett. **383** (2004) 215.

[14] H. Zhang, O. Kullie and D. Kolb, J. Phys. B **37** (2004) 905.

[15] H. Zhang, H. J. Luo, J. Kolb, O. Kullie and D. Kolb, J. Phys. B **38** (2005) 2955.

[16] O. Kullie and D. Kolb, Eur. Phys. J. D **17** (2001) 167.

[17] O. Kullie and D. Kolb, J. Phys. B: At. Mol. Opt. Phys. **36** (2003) 4361.

[18] W. -D. Sepp, D. Kolb, W. Sengler, H. Hartung and B. Fricke, Phys. Rev. A **33** (1986) 3679.

[19] T. Baştuğ, D. Heinemann, W. -D. Sepp, D. Kolb and B. Fricke, Chem. Phys. Lett. **211** (1993) 119.

[20] T. Baştuğ, W. -D. Sepp, D. Kolb, B. Fricke, E. J. Baerends, and G. Te. Velde, J. Phys. B **28** (1995) 2325.

[21] J. Anton, T. Jacob, and B. Fricke, E. Engel, Phys. Rev. Lett. **89** (2002) 213001.

[22] W. -D. Sepp and B. Fricke, Physica Scripta **36** (1987) 268.

[23] F. Wang, W. Liu , Chem. Phys. **311** (2005) 63.

[24] O. Kullie , H. Zhang, and D. Kolb, Chem. Phys. accepted (2008) .

[25] P. Kürpick, W. -D. Sepp, and B. Fricke, Phys. Rev. A **51** (1995) 3693.

[26] J. Anton, K. Schulze, P. Křpick, W. -D. Sepp, and B. Fricke, Hyperfine Interact. **108** (1997) 89.

[27] K. Schulze, J. Anton, W. -D. Sepp, P. Kürpick, and B. Fricke, J. Phys. B **30** (1997) L67.

[28] K. Schulze, J. Anton, W. -D. Sepp, and B. Fricke, Phys. Rev. A **58** (1998) 1578.

[29] K. Schulze, J. Anton, W. -D. Sepp, and B. Fricke, Phys. Rev. A **58** (1998) 1578.

[30] F. A. Parpia, A. K. Mohanty, Chem. Phys. Let. **238** (1995) 209.

[31] L. LaJohn, J. D. Talman, Chem. Phys. Lett. **189** (1992) 383.

[32] L. Yang, D. Heinemann, and D. Kolb, Phys. Rev. A **48** (1993) 2700.

[33] C. Düsterhöft, L. Yang, D. Heinemann, and D. Kolb, Chem. Phys. Lett. **229** (1994) 667.

[34] C. Düsterhöft, D. Heinemann, D. Kolb, Chem. Phys. Lett. **296** (1998) 77.

[35] O. Kullie, C. Düsterhöft, D. Kolb, Chem. Phys. Lett. **314** (1999) 307.

[36] J. Dolbeault, M. J. Esteban, E. Séré, Int. J. Quan. Chem. **93** (2003) 149.

[37] W. Liu, C. van Wüllen , J. Chem. Phys. **113** (2000) 2506.

[38] L. Yang, D. Heinemann, and D. Kolb, Chem. Phys. Lett. **178** (1991) 213.

[39] J. Anton and B. Fricke, E. Engel, Phys. Rev. A **69** (2004) 012505.

[40] C. Düsterhöft, Ph.D. thesis, Universität Gesamthochschule Kassel, Dezember 1996.

[41] O. Kullie , H. Zhang, J. Kolb and D. Kolb, J. Chem. Phys. **125** (2006) 244303.

[42] K. E. Atkinson, *An Introduction to Numerical Analysis* (John Wiley and Sons, New York, 1978).

[43] F. Rosicky, F. Mark, Theoret. Chim. Acta **54** (1979) 35.

[44] P. Hohenberg and W. Kohn , Phys. Rev. **136** (1964) 864.

[45] W. Kohn and L. J. Sham , Phys. Rev. A **140** (1965) 1133.

[46] S. H. Vosko, L.Wilk, and Nusair , Can. J. Phys. **58** (1980) 1200.

[47] A.K. Rajagopal , J. Phys. C **11** (1978) L943.

[48] A. D. Becke , Phys. Rev. A **38** (1988) 3098.

[49] J. P. Perdew , Phys. Rev. B **33** (1986) 8822.

[50] S. Varga, B. Fricke, etc., J. Chem. Phys. **112** (2000) 3499.

[51] B.I. Dunlap, J. W. D. Conolly, and J. R. Sabin , J. Chem. Phys. **71** (1979) 4993.

[52] C. Sarpe-Tudoran, Ph.D. thesis, University Kassel, Kassel , Juni 2004.

[53] B. A. Hess, U. Kaldor , J. Chem. Phys. **112** (2000) 1809.

[54] D. R. Lide, *CRC Handbook of Chemistry and Physics* (CRS Press, Taylor & Francis, USA, 86th edition, 2005-2006).

[55] G. Te Velde and E. J. Baerends, J. Compt. Phys. **99** (1992) 84.

[56] S. Varga, E. Engel; W. D. Sepp; and B. Fricke , Phys. Rev. A **59** (1999) 4288.

[57] E. Engel , private communication

[58] W. Liu, C. van Wüllen , J. Chem. Phys. **110** (1999) 3730.

[59] W. -D. Sepp, B. Fricke and T. Morović , Phys. Lett. **81** (1981) 258.

Appendix A

Kinetic Matrix Element

A.1 Traditional Four-Spinor LCAO

Because of using numerical atomic basis, the kinetic operator is defined by atomic kinetic operator acting on atomic basis, namely, $T\phi_i$. The kinetic matrix element will be derived by following express:

$$
\begin{aligned}
\langle \psi \,|\, T\psi \rangle &= \sum_j \sum_k a_j a_k \langle \begin{pmatrix} \phi_{j+} \\ \phi_{j-} \end{pmatrix} \,|\, T \begin{pmatrix} \phi_{k+} \\ \phi_{k-} \end{pmatrix} \rangle \\
&= \sum_j \sum_k a_j a_k \langle \begin{pmatrix} \phi_{j+} \\ \phi_{j-} \end{pmatrix} \,|\, (\varepsilon_k^{AO} - V_k^{AO}) \begin{pmatrix} \phi_{k+} \\ \phi_{k-} \end{pmatrix} \rangle
\end{aligned}
\tag{A.1}
$$

A.2 TVB LCAO

One could separate the small component of molecular wavefunction as following:

$$
\begin{aligned}
\psi_- &= \sum_i a_i \frac{L\phi_{i+}}{(E_0 + 2mc^2 - V^{MO})} \\
&= \sum_i a_i \frac{L\phi_{i+}}{(\varepsilon_i^{AO} + 2mc^2 - V_i^{AO})} \frac{(\varepsilon_i^{AO} + 2mc^2 - V_i^{AO})}{(E_0 + 2mc^2 - V^{MO})} \\
&= \sum_i a_i \phi_{i-}(1 + \frac{(\varepsilon_i^{AO} - E_0 + V^{MO} - V_i^{AO})}{(E_0 + 2mc^2 - V^{MO})}) \\
&= \sum_i a_i \phi_{i-}(1 + g_i(E_0))
\end{aligned}
$$

$$= \sum_i a_i \tilde{\phi}_{i-} \tag{A.2}$$

where $g_i(E_0)$ is for abbreviation

$$g_i(E_0) = \frac{(\varepsilon_i^{AO} - E_0 + V^{MO} - V_i^{AO})}{(E_0 + 2mc^2 - V^{MO})} \tag{A.3}$$

The kinetic matrix is shown here. The overlapping and potential matrices are similar and simple. $\delta_i = b_i - a_i$ is used for convenience.

$$
\begin{aligned}
\langle \psi \mid T\psi \rangle &= \sum_j \sum_k \langle \begin{pmatrix} a_j\phi_{j+} \\ b_j\tilde{\phi}_{j-} \end{pmatrix} \mid T \begin{pmatrix} a_k\phi_{k+} \\ b_k\tilde{\phi}_{k-} \end{pmatrix} \rangle \\
&= \sum_j \sum_k \langle \begin{pmatrix} a_j\phi_{j+} \\ b_j\phi_{j-} \end{pmatrix} + \begin{pmatrix} 0 \\ b_j\phi_{j-}g_j(E_0) \end{pmatrix} \mid T \left(\begin{pmatrix} a_k\phi_{k+} \\ b_k\phi_{k-} \end{pmatrix} + \begin{pmatrix} 0 \\ b_k\phi_{k-}g_k(E_0) \end{pmatrix} \right) \rangle \\
&= \sum_j \sum_k \langle \begin{pmatrix} a_j\phi_{j+} \\ (a_j + \delta_j)\phi_{j-} \end{pmatrix} + \begin{pmatrix} 0 \\ (a_j + \delta_j)\phi_{j-}g_j(E_0) \end{pmatrix} \mid \\
&\quad T \left(\begin{pmatrix} a_k\phi_{k+} \\ (a_k + \delta_k)\phi_{k-} \end{pmatrix} + \begin{pmatrix} 0 \\ (a_k + \delta_k)\phi_{k-}g_k(E_0) \end{pmatrix} \right) \rangle \\
&= \sum_j \sum_k \langle \begin{pmatrix} a_j\phi_{j+} \\ (a_j + \delta_j)\phi_{j-} \end{pmatrix} \mid T \left(\begin{pmatrix} a_k\phi_{k+} \\ (a_k + \delta_k)\phi_{k-} \end{pmatrix} \right) \rangle \\
&\quad + \sum_j \sum_k \langle \begin{pmatrix} a_j\phi_{j+} \\ (a_j + \delta_j)\phi_{j-} \end{pmatrix} \mid T \left(\begin{pmatrix} 0 \\ (a_k + \delta_k)\phi_{k-}g_k(E_0) \end{pmatrix} \right) \rangle \\
&\quad + \sum_j \sum_k \langle \begin{pmatrix} 0 \\ (a_j + \delta_j)\phi_{j-}g_j(E_0) \end{pmatrix} \mid T \left(\begin{pmatrix} a_k\phi_{k+} \\ (a_k + \delta_k)\phi_{k-} \end{pmatrix} \right) \rangle \\
&\quad + \sum_j \sum_k \langle \begin{pmatrix} 0 \\ (a_j + \delta_j)\phi_{j-}g_j(E_0) \end{pmatrix} \mid T \left(\begin{pmatrix} 0 \\ (a_k + \delta_k)\phi_{k-}g_k(E_0) \end{pmatrix} \right) \rangle \tag{A.4}
\end{aligned}
$$

- first term

$$
\begin{aligned}
&\sum_j \sum_k \langle \begin{pmatrix} a_j\phi_{j+} \\ (a_j + \delta_j)\phi_{j-} \end{pmatrix} \mid T \begin{pmatrix} a_k\phi_{k+} \\ (a_k + \delta_k)\phi_{k-} \end{pmatrix} \rangle \\
&= \sum_j \sum_k a_j a_k \langle \begin{pmatrix} \phi_{j+} \\ \phi_{j-} \end{pmatrix} \mid T \begin{pmatrix} \phi_{k+} \\ \phi_{k-} \end{pmatrix} \rangle + \sum_j \sum_k a_j \delta_k \langle T \begin{pmatrix} \phi_{j+} \\ \phi_{j-} \end{pmatrix} \mid \begin{pmatrix} 0 \\ \phi_{k-} \end{pmatrix} \rangle
\end{aligned}
$$

$$+\sum_j \sum_k \delta_j a_k \langle \begin{pmatrix} 0 \\ \phi_{j-} \end{pmatrix} \mid T \begin{pmatrix} \phi_{k+} \\ \phi_{k-} \end{pmatrix} \rangle + \sum_j \sum_k \delta_j \delta_k \langle \begin{pmatrix} 0 \\ \phi_{j-} \end{pmatrix} \mid T \begin{pmatrix} 0 \\ \phi_{k-} \end{pmatrix} \rangle$$

$$= \sum_j \sum_k a_j a_k \langle \begin{pmatrix} \phi_{j+} \\ \phi_{j-} \end{pmatrix} \mid (\varepsilon_k^{AO} - V_k^{AO}) \begin{pmatrix} \phi_{k+} \\ \phi_{k-} \end{pmatrix} \rangle$$

$$+ \sum_j \sum_k a_j \delta_k \langle (\varepsilon_j^{AO} - V_j^{AO}) \begin{pmatrix} \phi_{j+} \\ \phi_{j-} \end{pmatrix} \mid \begin{pmatrix} 0 \\ \phi_{k-} \end{pmatrix} \rangle$$

$$+ \sum_j \sum_k \delta_j a_k \langle \begin{pmatrix} 0 \\ \phi_{j-} \end{pmatrix} \mid (\varepsilon_k^{AO} - V_k^{AO}) \begin{pmatrix} \phi_{k+} \\ \phi_{k-} \end{pmatrix} \rangle$$

$$+ \sum_j \sum_k \delta_j \delta_k (-2mc^2) \langle \begin{pmatrix} 0 \\ \phi_{j-} \end{pmatrix} \mid \begin{pmatrix} 0 \\ \phi_{k-} \end{pmatrix} \rangle \tag{A.5}$$

- second term

$$\sum_j \sum_k \langle \begin{pmatrix} a_j \phi_{j+} \\ (a_j + \delta_j)\phi_{j-} \end{pmatrix} \mid T \begin{pmatrix} 0 \\ (a_k + \delta_k)\phi_{k-} g_k(E_0) \end{pmatrix} \rangle$$

$$= \sum_j \sum_k a_j (a_k + \delta_k) \langle T \begin{pmatrix} \phi_{j+} \\ \phi_{j-} \end{pmatrix} \mid \begin{pmatrix} 0 \\ \phi_{k-} g_k(E_0) \end{pmatrix} \rangle$$

$$+ \sum_j \sum_k \delta_j (a_k + \delta_k) \langle \begin{pmatrix} 0 \\ \phi_{j-} \end{pmatrix} \mid T \begin{pmatrix} 0 \\ \phi_{k-} g_k(E_0) \end{pmatrix} \rangle$$

$$= \sum_j \sum_k a_j (a_k + \delta_k) \langle (\varepsilon_j^{AO} - V_j^{AO}) \begin{pmatrix} \phi_{j+} \\ \phi_{j-} \end{pmatrix} \mid \begin{pmatrix} 0 \\ \phi_{k-} g_k(E_0) \end{pmatrix} \rangle$$

$$+ \sum_j \sum_k \delta_j (a_k + \delta_k)(-2mc^2) \langle \begin{pmatrix} 0 \\ \phi_{j-} \end{pmatrix} \mid \begin{pmatrix} 0 \\ \phi_{k-} g_k(E_0) \end{pmatrix} \rangle \tag{A.6}$$

- third term

$$\sum_j \sum_k \langle \begin{pmatrix} 0 \\ (a_j + \delta_j)\phi_{j-} g_j(E_0) \end{pmatrix} \mid T \begin{pmatrix} a_k \phi_{k+} \\ (a_k + \delta_k)\phi_{k-} \end{pmatrix} \rangle$$

$$= \sum_j \sum_k (a_j + \delta_j) a_k \langle \begin{pmatrix} 0 \\ \phi_{j-} g_j(E_0) \end{pmatrix} \mid T \begin{pmatrix} \phi_{k+} \\ \phi_{k-} \end{pmatrix} \rangle$$

$$+ \sum_j \sum_k (a_j + \delta_j) \delta_k \langle \begin{pmatrix} 0 \\ \phi_{j-} g_j(E_0) \end{pmatrix} \mid T \begin{pmatrix} 0 \\ \phi_{k-} \end{pmatrix} \rangle$$

$$\begin{aligned}
= \ & \sum_j \sum_k (a_j + \delta_j) a_k \langle \begin{pmatrix} 0 \\ \phi_{j-} g_j(E_0) \end{pmatrix} | \ (\varepsilon_k^{AO} - V_k^{AO}) \begin{pmatrix} \phi_{k+} \\ \phi_{k-} \end{pmatrix} \rangle \\
& + \sum_j \sum_k (a_j + \delta_j) \delta_k (-2mc^2) \langle \begin{pmatrix} 0 \\ \phi_{j-} g_j(E_0) \end{pmatrix} | \begin{pmatrix} 0 \\ \phi_{k-} \end{pmatrix} \rangle \qquad \text{(A.7)}
\end{aligned}$$

- fourth term

$$\begin{aligned}
& \sum_j \sum_k \langle \begin{pmatrix} 0 \\ (a_j + \delta_j) \phi_{j-} g_j(E_0) \end{pmatrix} | \ T \begin{pmatrix} 0 \\ (a_k + \delta_k) \phi_{k-} g_k(E_0) \end{pmatrix} \rangle \\
= \ & \sum_j \sum_k (a_j + \delta_j)(a_k + \delta_k)(-2mc^2) \langle \begin{pmatrix} 0 \\ \phi_{j-} g_j(E_0) \end{pmatrix} | \begin{pmatrix} 0 \\ \phi_{k-} g_k(E_0) \end{pmatrix} \rangle \ \text{(A.8)}
\end{aligned}$$

A.3   TVDB LCAO

Similar as TV balance, the small component of molecular wavefunction is formulated this way:

$$\begin{aligned}
\psi_- \ &= \ \sum_i a_i \frac{L\phi_{i+}}{(E_i + 2mc^2 - V^{MO})} + \sum_i b_i \frac{L\phi_{i+}}{(E_i + 2mc^2 - V^{MO})(E_0 + 2mc^2 - V^{MO})} \\
&= \ \sum_i a_i \phi_{i-}(1 + g_i(E_i)) + \sum_i b_i \phi_{i-} h_i(E_i, E_0) \\
&= \ \sum_i a_i \tilde{\phi}_{i-} + \sum_i b_i \phi_{i-} h_i(E_i, E_0) \qquad \text{(A.9)}
\end{aligned}$$

$$g_i(E_i) \ = \ \frac{(\varepsilon_i^{AO} - E_i + V^{MO} - V_i^{AO})}{(E_i + 2mc^2 - V^{MO})} \qquad \text{(A.10)}$$

$$h_i(E_i, E_0) \ = \ \frac{(\varepsilon_i^{AO} + 2mc^2 - V_i^{AO})}{(E_i + 2mc^2 - V^{MO})(E_0 + 2mc^2 - V^{MO})} \qquad \text{(A.11)}$$

$$\begin{aligned}
\langle \psi | T\psi \rangle \ &= \ \sum_j \sum_k \langle \begin{pmatrix} a_j \phi_{j+} \\ a_j \tilde{\phi}_{j-} + b_j \phi_{j-} h_j(E_j, E_0) \end{pmatrix} | \ T \begin{pmatrix} a_k \phi_{k+} \\ a_k \tilde{\phi}_{k-} + b_k \phi_{k-} h_k(E_k, E_0) \end{pmatrix} \rangle \\
&= \ \sum_j \sum_k \langle \begin{pmatrix} a_j \phi_{j+} \\ a_j \phi_{j-} \end{pmatrix} + \begin{pmatrix} 0 \\ a_j \phi_{j-} g_j(E_j) + b_j \phi_{j-} h_j(E_j, E_0) \end{pmatrix} |
\end{aligned}$$

$$T\left(\left(\begin{array}{c} a_k\phi_{k+} \\ a_k\phi_{k-} \end{array}\right) + \left(\begin{array}{c} 0 \\ a_k\phi_{k-}g_k(E_k) + b_k\phi_{k-}h_k(E_k, E_0) \end{array}\right)\right)\rangle$$

$$= \sum_j\sum_k\langle\left(\begin{array}{c} a_j\phi_{j+} \\ a_j\phi_{j-} \end{array}\right) \mid T\left(\begin{array}{c} a_k\phi_{k+} \\ a_k\phi_{k-} \end{array}\right)\rangle$$

$$+ \sum_j\sum_k\langle\left(\begin{array}{c} a_j\phi_{j+} \\ a_j\phi_{j-} \end{array}\right) \mid T\left(\begin{array}{c} 0 \\ a_k\phi_{k-}g_k(E_k) + b_k\phi_{k-}h_k(E_k, E_0) \end{array}\right)\rangle$$

$$+ \sum_j\sum_k\langle\left(\begin{array}{c} 0 \\ a_j\phi_{j-}g_j(E_j) + b_j\phi_{j-}h_j(E_j, E_0) \end{array}\right) \mid T\left(\begin{array}{c} a_k\phi_{k+} \\ a_k\phi_{k-} \end{array}\right)\rangle$$

$$+ \sum_j\sum_k\langle\left(\begin{array}{c} 0 \\ a_j\phi_{j-}g_j(E_j) + b_j\phi_{j-}h_j(E_j, E_0) \end{array}\right) \mid$$

$$T\left(\begin{array}{c} 0 \\ a_k\phi_{k-}g_k(E_k) + b_k\phi_{k-}h_k(E_k, E_0) \end{array}\right)\rangle \tag{A.12}$$

- first term

$$\sum_j\sum_k\langle\left(\begin{array}{c} a_j\phi_{j+} \\ a_j\phi_{j-} \end{array}\right) \mid T\left(\begin{array}{c} a_k\phi_{k+} \\ a_k\phi_{k-} \end{array}\right)\rangle$$

$$= \sum_j\sum_k a_j a_k\langle\left(\begin{array}{c} \phi_{j+} \\ \phi_{j-} \end{array}\right) \mid (\varepsilon_k^{AO} - V_k^{AO})\left(\begin{array}{c} \phi_{k+} \\ \phi_{k-} \end{array}\right)\rangle \tag{A.13}$$

- second term

$$\sum_j\sum_k\langle\left(\begin{array}{c} a_j\phi_{j+} \\ a_j\phi_{j-} \end{array}\right) \mid T\left(\begin{array}{c} 0 \\ a_k\phi_{k-}g_k(E_k) + b_k\phi_{k-}h_k(E_k, E_0) \end{array}\right)\rangle$$

$$= \sum_j\sum_k a_j a_k\langle(\varepsilon_j^{AO} - V_j^{AO})\left(\begin{array}{c} \phi_{j+} \\ \phi_{j-} \end{array}\right) \mid \left(\begin{array}{c} 0 \\ \phi_{k-}g_k(E_k) \end{array}\right)\rangle$$

$$+ \sum_j\sum_k a_j b_k\langle(\varepsilon_j^{AO} - V_j^{AO})\left(\begin{array}{c} \phi_{j+} \\ \phi_{j-} \end{array}\right) \mid \left(\begin{array}{c} 0 \\ \phi_{k-}h_k(E_k, E_0) \end{array}\right)\rangle \tag{A.14}$$

- third term

$$\sum_j\sum_k\langle\left(\begin{array}{c} 0 \\ a_j\phi_{j-}g_j(E_j) + b_j\phi_{j-}h_j(E_j, E_0) \end{array}\right) \mid T\left(\begin{array}{c} a_k\phi_{k+} \\ a_k\phi_{k-} \end{array}\right)\rangle$$

$$= \sum_j\sum_k a_j a_k\langle\left(\begin{array}{c} 0 \\ \phi_{j-}g_j(E_j) \end{array}\right) \mid (\varepsilon_k^{AO} - V_k^{AO})\left(\begin{array}{c} \phi_{k+} \\ \phi_{k-} \end{array}\right)\rangle$$

$$+ \sum_j\sum_k b_j a_k\langle\left(\begin{array}{c} 0 \\ \phi_{j-}h_j(E_j, E_0) \end{array}\right) \mid (\varepsilon_k^{AO} - V_k^{AO})\left(\begin{array}{c} \phi_{k+} \\ \phi_{k-} \end{array}\right)\rangle \tag{A.15}$$

- fourth term

$$
\sum_j \sum_k \langle \begin{pmatrix} 0 \\ a_j\phi_{j-}g_j(E_j) + b_j\phi_{j-}h_j(E_j, E_0) \end{pmatrix} \mid T \begin{pmatrix} 0 \\ a_k\phi_{k-}g_k(E_k) + b_k\phi_{k-}h_k(E_k, E_0) \end{pmatrix} \rangle
$$

$$
= \sum_j \sum_k (-2mc^2) \langle \begin{pmatrix} 0 \\ a_j\phi_{j-}g_j(E_j) + b_j\phi_{j-}h_j(E_j, E_0) \end{pmatrix} \mid
$$

$$
\begin{pmatrix} 0 \\ a_k\phi_{k-}g_k(E_k) + b_k\phi_{k-}h_k(E_k, E_0) \end{pmatrix} \rangle \tag{A.16}
$$

A.4   Minimax Two-Spinor LCAO

$$
I = \langle \psi_+ \mid (V^{MO} - E)\psi_+ \rangle + \langle \psi_- \mid L\psi_+ \rangle \tag{A.17}
$$

with

$$
\psi_- = \frac{L\psi_+}{(E + 2mc^2 - V^{MO})}
$$

$$
= \sum_k a_k\phi_{k-}(1 + g_k(E)) \tag{A.18}
$$

$$
g_k(E) = \frac{(\varepsilon_k^{AO} - E + V^{MO} - V_k^{AO})}{(E + 2mc^2 - V^{MO})} \tag{A.19}
$$

and

$$
\psi_+ = \sum_k a_k\phi_{k+} \tag{A.20}
$$

The direct use of the following numerical definition spoils the quadratic error dependence of energies and introduces a linear error term as in the approximate wave functions (atomic orbital $1s_{\frac{1}{2}}$ of Th_2^{179+} as a test).

$$
T\phi_k = \begin{pmatrix} 0 & L^\dagger \\ L & -2mc^2 \end{pmatrix} \begin{pmatrix} \phi_{k+} \\ \phi_{k-} \end{pmatrix} \tag{A.21}
$$

$$
L\phi_{k+} = (T\phi_k)_- + 2mc^2\phi_{k-} \tag{A.22}
$$

we use an equation to avoid this numerical definition:

$$
\begin{aligned}
\langle \psi \mid T\phi_k \rangle &= \langle \psi_+ \mid L^\dagger \phi_{k-} \rangle + \langle \psi_- \mid L\phi_{k+} - 2mc^2 \phi_{k-} \rangle \\
&= \langle L\psi_+ \mid \phi_{k-} \rangle + \langle \psi_- \mid L\phi_{k+} - 2mc^2 \phi_{k-} \rangle \\
&= \langle (E + 2mc^2 - V^{MO})\psi_- \mid \phi_{k-} \rangle + \langle \psi_- \mid L\phi_{k+} - 2mc^2 \phi_{k-} \rangle \\
&= \langle (E - V^{MO})\psi_- \mid \phi_{k-} \rangle + \langle \psi_- \mid L\phi_{k+} \rangle
\end{aligned} \tag{A.23}
$$

with

$$
\langle \psi \mid T\phi_k \rangle = \langle \psi \mid (\varepsilon_k^{AO} - V_k^{AO})\phi_k \rangle \tag{A.24}
$$

one gets:

$$
\langle \psi_- \mid L\phi_{k+} \rangle = \langle \psi \mid (\varepsilon_k^{AO} - V_k^{AO})\phi_k \rangle - \langle (E - V^{MO})\psi_- \mid \phi_{k-} \rangle \tag{A.25}
$$

That is what I need to use for the minimax functional:

$$
\begin{aligned}
I &= \langle \psi_+ \mid (V^{MO} - E)\psi_+ \rangle + \langle \psi_- \mid L\psi_+ \rangle \\
&= \langle \psi_+ \mid (V^{MO} - E)\psi_+ \rangle + \sum_k a_k \langle \psi_- \mid L\phi_{k+} \rangle \\
&= \langle \psi_+ \mid (V^{MO} - E)\psi_+ \rangle + \\
&\quad \sum_k a_k (\langle \psi \mid (\varepsilon_k^{AO} - V_k^{AO})\phi_k \rangle - \langle (E - V^{MO})\psi_- \mid \phi_{k-} \rangle) \\
&= \langle \psi_+ \mid (V^{MO} - E)\psi_+ \rangle + \sum_k a_k (\langle \psi_+ \mid (\varepsilon_k^{AO} - V_k^{AO})\phi_{k+} \rangle \\
&\quad + \langle \psi_- \mid (\varepsilon_k^{AO} - V_k^{AO})\phi_{k-} \rangle - \langle (E - V^{MO})\psi_- \mid \phi_{k-} \rangle) \\
&= \sum_j \sum_k a_j a_k (\langle \phi_{j+} \mid ((V^{MO} - E) + (\varepsilon_k^{AO} - V_k^{AO}))\phi_{k+} \rangle \\
&\quad + \langle \phi_{j-}(1 + g_j(E)) \mid ((\varepsilon_k^{AO} - V_k^{AO}) - (E - V^{MO}))\phi_{k-} \rangle)
\end{aligned} \tag{A.26}
$$

A.5 Conversion of units:

$$
\begin{aligned}
1 \ a.u. &= 2 \ Rydberg \\
1 \ a.u. &= 52.917726 \ pm \\
1 \ a.u. &= 27.21165 \ eV
\end{aligned}
$$

$$\tag{A.27}$$

Acknowledgments

Eidesstattliche Erklärung

Hiermit versichere ich, dass ich die vorliegende Dissertation selbständig und ohne unerlaubte Hilfe angefertigt habe. Andere als in der Arbeit angegebene Hilfsmittel wurden von mir nicht benutzt. Alle Stellen, die wörtlich oder sinngemäß aus veröffentlichen oder unveröffentlichen Schriften entnommen sind, habe ich als solche gekennzeichnet. Kein Teil dieser Dissertation ist in einem anderen Promotions- oder Habilitationsverfahren verwendet.

Kassel, den 25. November 2008

Curriculum Vitae

Name: Hui Zhang

male

Feb. 24, 1973 born in Emei, Sichuan, China

1979-1984 School pupil, element school of Emei 739, Emei, China

1984-1990 School pupil, high school of Emei 739, Emei, China

1990-1994 University student (Bachelor of Science), Department of applied physics, Sichuan University, China

1994-1997 Postgraduate (Master of Science), Department of applied physics, Sichuan University, China

1997-2002 Lecturer, Department of applied physics, Sichuan University, China

2002-now Scientific collaborator, Department of Physics, University of Kassel, Kassel, Germany